Stony Brook University

The investigation of enoyl-CoA hydratases in cholesterol metabolism of *Mycobacterium tuberculosis*

A Thesis Presented

by

Jungwon Jang

to

The Graduate School

in Partial Fulfillment of the

Requirements

for the Degree of

Master of Science

in

Chemistry

Stony Brook University

August 2016

Stony Brook University

The Graduate School

Jungwon Jang

We, the thesis committee for the above candidate for the

Master of Science degree, hereby recommend

acceptance of this thesis.

Nicole S. Sampson, Ph.D. – Thesis Advisor
Department of Chemistry

Scott Laughlin, Ph.D. – Chairperson
Department of Chemistry

Dale G. Drueckhammer, Ph.D. - Third member
Department of Chemistry

This thesis is accepted by the Graduate School

Nancy Goroff
Interim Dean of the Graduate School

Abstract of the Thesis

The investigation of enoyl-CoA hydratases in cholesterol metabolism of *Mycobacterium tuberculosis*

by

Jungwon Jang

Master of Science

in

Chemistry

Stony Brook University

2016

Mycobacterium tuberculosis (*Mtb*) is the bacterium that causes tuberculosis (TB) in humans. TB is one of the deadliest infectious diseases in the world. *Mtb* resides in the lipid-enriched environment of the host and metabolizes cholesterol as a carbon source using its own enzymes. Among the total 4000 genes of *Mtb*, 250 genes correlate to the enzymatic reactions of lipid utilization.

The degradation of cholesterol side chain is characterized by three cycles of β-oxidation. Each of the β-oxidation cycles involves hydration of the dehydrogenated cholesterol intermediate substrate. Rv3538 and EchA19 are expected to function as an enoyl-CoA hydratase in the cholesterol metabolism of *Mtb*. In this project, the hydratase candidates Rv3538 and EchA19 were expressed and tested with the dehydrogenated cholesterol intermediates of the β-oxidation cycles. *Rv3538*, *echA19*, and *chsH1-chsH2* are controlled by same regulator of KstR1. The

enoyl-CoA hydratase candidates of Rv3538, EchA19, and ChsH1-ChsH2 are predicted to be involved in similar enzymatic reactions. The enoyl-CoA hydratase, ChsH1-ChsH2, was previously identified to hydrate the cholesterol intermediate of the 3rd β-oxidation cycle. The substrate 3-oxo-chol-4-en-24-oyl-CoA (3-OCO-CoA) is involved in the 2nd β-oxidation cycle. The target protein of Rv3538 was investigated for the hydration of the 2nd β-oxidation. The 1st β-oxidation cycle contains 3-oxo-cholest-4-en-26-oyl-CoA (3-OCS-CoA) as a substrate. The enzymatic reaction of EchA19 and dehydrogenated 3-OCS-CoA was monitored using MALDI TOF mass spectroscopy.

EchA13, *fadE17*, and *fadE18* are members of the Mce3R regulon. The substrate of EchA13 is predicted to be a product of the enzymatic reaction of FadE17 or FadE18. The investigation about EchA13 would give valuable information to identify FadE17 and FadE18 in the future. EchA13 is expected to function as an enoyl-CoA hydratase for *Mtb*. EchA13 was expressed and tested with the substrate of C12-enoyl-CoA. The enzymatic reaction was monitored by MALDI TOF mass spectroscopy.

Table of Contents

List of Figures/Tables

Figures

Tables

List of Abbreviations

2×YT	2× yeast extract tryptone broth
3-OCO-CoA	3-oxo-chol-4-en-24-oyl-CoA
3-OCS-CoA	3-oxo-cholest-4-en-26-oyl-CoA
ACN	acetonitrile
APS	ammonium persulfate
C12-enoyl-CoA	trans-dodec-2-enoyl-CoA
CoA	coenzyme A
DHB	2,5-dihydroxybenzoic acid
DMSO	dimethyl sulfoxide
dNTP	deoxynucleotide
EchA	enoyl-CoA hydratase
E. coli	*Escherichia coli*
EEA1	early endosomal antigen
Fad	fatty acid degrading

Hydratase	enoyl-CoA hydratase
HEPES	4-(2-hydroxyethyl)-1-piperazineethanesulfonic acid
HIV	immunodeficiency virus
IPTG	β-D-1-thiogalactopyranoside
kDa	kilodalton
LB	Luria-Bertani
MALDI	matrix assisted laser desorption/ionization
MDR-TB	multidrug-resistant TB
MS	mass spectrometry
MWCO	molecular weight cut off
Mtb	*Mycobacterium tuberculosis*
OD	optical density
PCR	Polymerase chain reaction
PI3P	phosphatidyl inositol 3-phospate
rpm	revolutions per minute
SDS-PAGE	sodium dodecyl sulfate polyacrylamide gel electrophoresis

TAE	tris-acetate EDTA
TB	tuberculosis
TCEP	tris-2-carboxyethylphosphine
TEMED	tetramethylenediamine
TFA	trifluoroacetic acid
TNF	tumor necrosis factor
TRIS	tris(hydroxymethyl)aminomethane
UV	ultraviolet visible
WHO	World Health Organization
XDR	extensively drug-resistant

Chapter 1. Introduction

1-1. Tuberculosis and *Mycobacterium tuberculosis*

Tuberculosis (TB) causes lung disease in humans. It spreads from person to person through the air. TB makes the person become sick and leads to death. The lung disease is the most common clinical diagnosis from TB (1). This disease is fatal to the patient without medical treatment. The infection of TB also affects the central nervous system. The risk of tuberculosis meningitis is increased for children under 5 years old and human immunodeficiency virus (HIV) co-infected patients (1). A *Mycobacterium tuberculosis* (*Mtb)* is a bacterium that causes TB in humans. It resides in a lipid environment in the host and survives with cholesterol from the human. It is expected that cholesterol metabolism of *Mtb* is important for the bacterium to survive in the host. The cholesterol metabolism of *Mtb* in the host is predicted to provide an energy source and lipid components for the bacterium. Therefore, identifying a way to inhibit and stop *Mtb* cholesterol metabolism will improve the treatment of TB in the future.

1-2. Statistics and treatment

TB is one of the deadliest infectious diseases in the world. The disease is spread from the infected patient to another person. According to the World Health Organization (WHO), 9.6 million people were infected with TB in 2014. Furthermore, 1.5 million died from the disease (10).

The standard protocol for TB therapy is treatment using five drugs for the first two months, and then using rifampicin and isoniazid for four months. However, the whole process

with current methods requires a long period of treatment. In addition, the medical methods cause many side effects as shown in table 1 (5).

First line drugs (Oral agents)	Major adverse reactions
Pyrazinamide	Gastrointestinal upset
Ethambutol	Decreased visual activity
Rifabutin	Hepatitis, fever, and flu-like syndrome
Isoniazid	Hepatitis, increasing hepatic enzymes
Streptomycin	Auditory and renal toxicity

Table 1 The first line drugs for TB therapy and their major side effects

Furthermore, the current standard protocol for TB is only applied for patients with non-resistant *Mtb* infection. About 3% of the new TB cases in the world are estimated to be multidrug-resistant TB (MDR-TB) (6). About 440,000 cases of MDR-TB were estimated in 2008 (2). Typically, the patients with MDR-TB have resistance to at least isoniazid and rifampicin, which are the most common effective anti-TB drugs (6). The second-line anti-TB drugs are likely to be effective for the treatment of MDR-TB, but they require at least 20 months of treatment (6).

Oral bacteriostatic second line drugs	Major adverse reactions
Para-aminosalicylic acid	Vomiting and diarrhea
Cycloserine	Psychosis and seizures
Terizidone	Depression, paranoia, and dizziness
Ethionamide	Gastrointestinal upset and bloating
Prothionamide	Nausea and vomiting

Table 2 The second line TB drugs and their major side effects

Moreover, as shown in table 2, the second line drugs for TB therapy also causes some side effects (13). The current treatment for MDR-TB shows higher rates of treatment failure and mortality. Furthermore, only a few countries obtained the medical treatment for MDR-TB (2).

Multidrug-resistant (MDR) and extensively drug-resistant (XDR) tuberculosis has emerged in the world (2). XDR tuberculosis is a type of TB that has a resistance even to the second-line TB drugs. The resistance of XDR tuberculosis emerges to at least three classes of second-line drugs. XDR tuberculosis is seriously fatal to the patients with HIV co-infection (12).

Additionally, the standard protocol for the treatment of TB worked only for the patient without HIV (5). TB became the second common infectious disease in the world causing death to the patients with HIV (1). It has been reported that about one million people suffered from HIV/TB co-infection (13). Eleven percent of new TB cases in 2000 are estimated as a co-infection of HIV (1). However, the current medical treatment for TB with HIV co-infection is toxic and expensive (13).

An effective medical treatment for the tuberculosis with antibiotic resistance for patients with HIV does not currently exist. The further information about the infectious process in *Mtb* that is closely related to cholesterol metabolism would provide valuable insight to a more effective TB therapy.

1-3. The infectious process of *Mtb*

Mtb is transmitted to the lung by an aerosol and resides in macrophages. (1). The bacteria spread when the infected person is coughing, sneezing, or talking. *Mtb* contained in an airborne droplet suspended in air exists for minutes to hours (1).

Macrophage is one of the immune cells that have a responsibility to protect human's body from pathogens. The pathogen that is engulfed by macrophage is normally digested by lysosome. Macrophages have a function to destroy any dead cells and foreign microbes (10). However, the hostile environment of the host macrophage is a key for the mechanism of *Mtb* to survive in the host. *Mtb* uses its pathogenic ability to resist attack from the human immune system (7). The infected macrophages in pathogenic mycobacteria prevent the phagosome to fuse to lysosome (10). Therefore, *Mtb* hides in macrophages and replicates itself unrestrictedly (1).

Although cell-mediated immune system develops in 2~8 weeks after the infection, *Mtb* keeps replicating in the lymphatic system (1). After the infection with *Mtb*, pulmonary granulomas are formed in the host (4). Then, the further replication is limited by activated T lymphocytes, and macrophages form granulomas. The center of *Mtb* is characterized as necrotic granulomas, and its presence is shown as a positive result in the tuberculin skin test (1). The granuloma is a compact aggregate of immune cells. However, it is known as a hallmark structure of TB infection that implicates innate immune mechanism of the infected granuloma (3). The local interaction between the host cells and the bacterium causes the granuloma to form with *Mtb* at the site of infection (11). The infected macrophage stimulates T lymphocytes and releases interferon Y. The interferon Y stimulates the infected macrophages to release tumor necrosis factor (TNF)-α that supports pathogen infected granuloma formation (1).

The granuloma with *Mtb* contains infected macrophages, and it is surrounded by foamy macrophages. The macrophage with *Mtb* forms a foam cell. The foamy macrophage is predicted to be an important tactic for survival of *Mtb* (11). The foam cell contains accumulated fatty substances such as cholesterol and lipid molecules. *Mtb* resides in the foam cell and shifts its metabolism process to a lipid-based mechanism. Therefore, the foamy macrophages are expected as a key participant during the infectious process of *Mtb* in the host.

1-4. Cholesterol metabolism of *Mtb*

Cholesterol metabolism is expected to be important for *Mtb* to survive in humans. It is known that *Mtb* lives in lipid-rich environment in the host, and the bacterium digests the substrate of cholesterol intermediate using its enzyme. The lipid components have essential roles in the mycobacterial cell wall. The mycobacterial virulence involving the biosynthesis of cell wall components has not yet been clearly identified (8). The lipid component influences the inflammatory response and disrupts the intracellular fate of pathogenic mycobacteria. Mycobacterial lipids have the innate ability to inhibit the fusion of the mycobacterial phagosome to lysosomes (8).

Mtb has an ability to disrupt maturation of phagosomes to phagolysosomes using lipid components. The early endosomal antigen (EEA1) interacts with phosphatidyl inositol 3-phospate (PI3P). PI3P is one of the key lipid effectors that controls membrane trafficking in the endolysosomal system. However, the generation of PI3P on the endosomal membrane is interrupted by mycobacteria, and it disrupts the delivery of phagosomes to lysosomes (9).

Mtb degrades cholesterol to acetate and propionate. It is previously found that *Mtb* uses cholesterol as a significant carbon source of propionate for survival of *Mtb*. The degradation of cholesterol is characterized by β-oxidation of the side chain (14).

In 1998, a total 4000 genes of *Mtb* were identified. At least 250 genes were identified in the lipid utilization of *Mtb*. The genes that are involved in lipid-metabolism pathways are predicted to function in infectious process of *Mtb* (15). Many genes that are involved in the degradation pathway of cholesterol have not been identified yet. In this project, the function of hydratases that are related to metabolism of cholesterol side chain is studied. The metabolism of cholesterol consists of three cycles. Figure 1 represents the steps of the cholesterol degradation and the substrates of the three cycles of the side chain degradation.

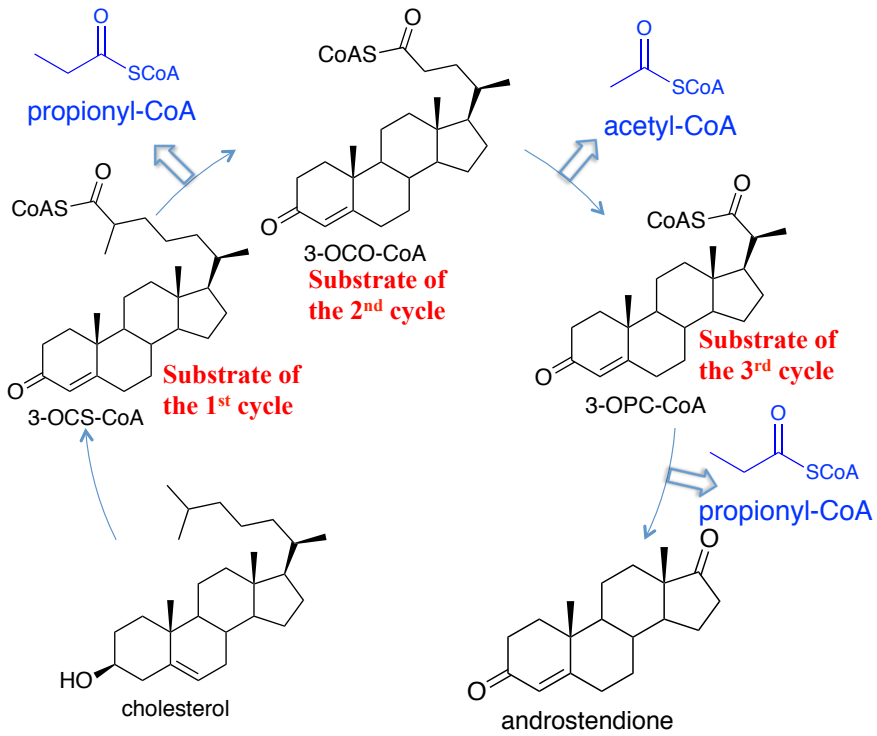

Figure 1 The process of cholesterol side chain degradation

As shown in figure 1, each of three cycles contains a different number of carbons in the side chain of the cholesterol intermediates. The degradation of the side chain consists of dehydrogenation of the substrate, followed by hydration to the double bond. In both of the first and third β-oxidation cycle contains the substrates with α-methyl branched acyl-CoAs. However, the substrate in the second cycle has a straight chain without methyl branch.

1-5. Specific aims

The purpose of this research project is to identify the function of the hydratase candidates with specific cholesterol intermediate substrates of *Mtb*. The aims of this project are expression and purification of the expected hydratases, and investigation of the enzymatic reaction of recombinant protein with the intermediate substrate of each β-oxidation cycle in cholesterol metabolism. The result will demonstrate whether the specific hydratase (Rv3538, EchA13, EchA19) functions within a particular cycle of the cholesterol metabolism.

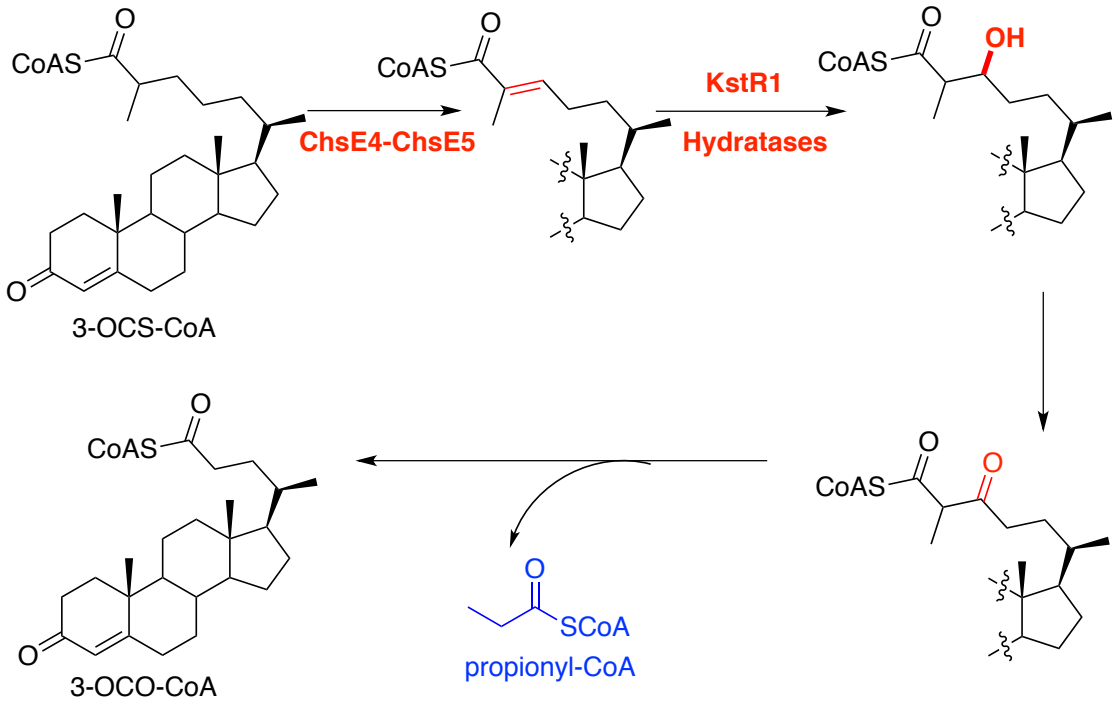

Figure 2 The mechanism of the first cycle of cholesterol metabolism in *Mtb*

Figure 2 represents the dehydrogenation and hydration of the 1st cycle of the side chain degradation of the cholesterol intermediate. As shown in figure 2, the 1st cycle substrate of 3-OCS-CoA was previously known to be dehydrogenated by ChsE4-ChsE5 (15). One of the hydratases in KstR1 regulon is expected to function in the hydration of the dehydrogenated substrate at the first cycle of the metabolism.

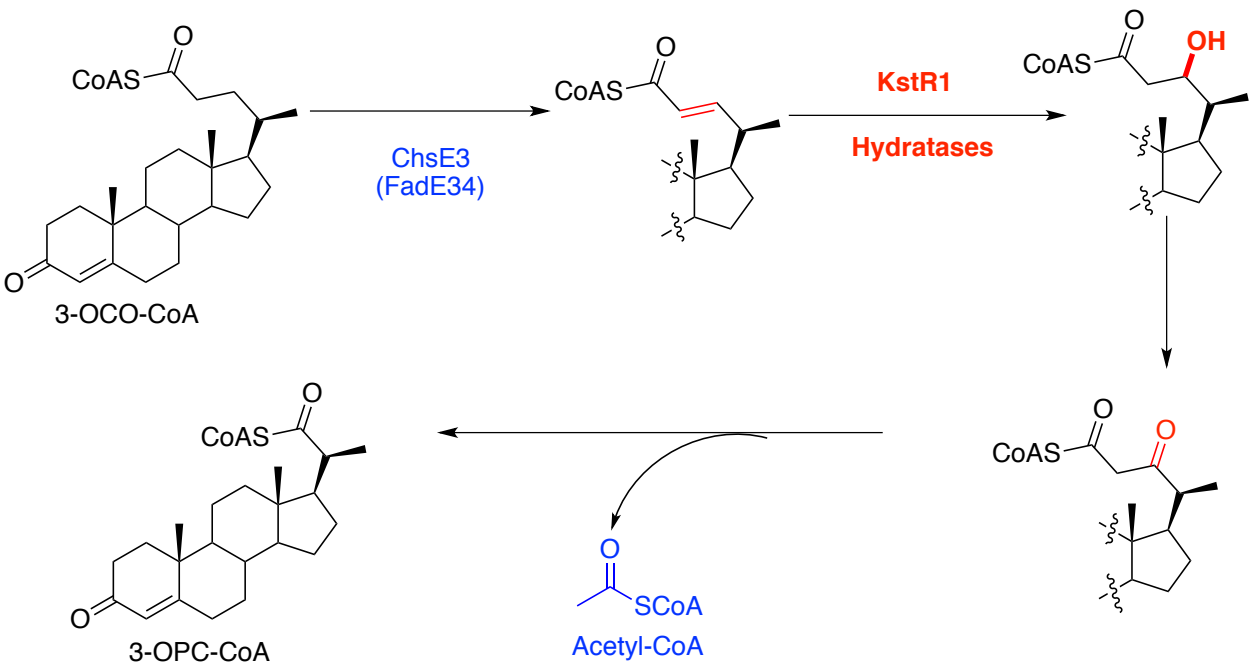

Figure 3 The mechanism of the second cycle of cholesterol metabolism in *Mtb*

Figure 3 shows the dehydrogenation and hydration of the side chain at the 2nd cycle of the cholesterol intermediate metabolism. *Rv3538* and *echA19* are in the same regulon as *chsH1-chsH2* called KstR1. The enzymes of Rv3538 and EchA19 that are correlated to KstR1 regulon are expected to be candidates for side chain metabolism.

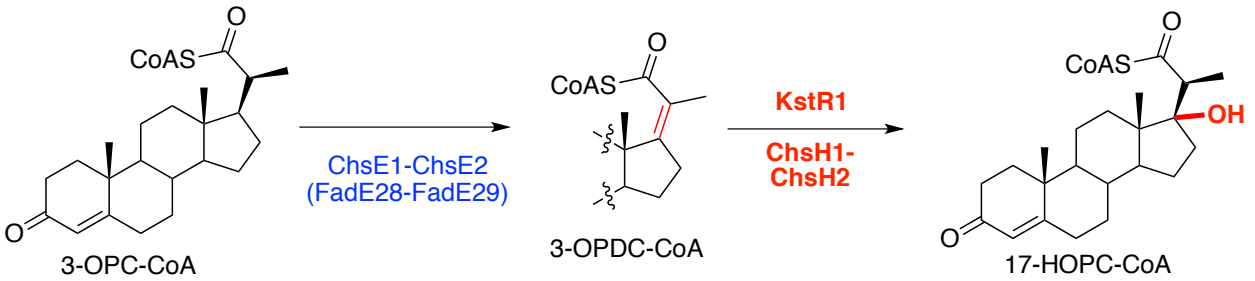

Figure 4 The mechanism of dehydrogenation and hydration at the third cycle of cholesterol metabolism in *Mtb*

Figure 4 demonstrates the dehydrogenation and hydration of the 3rd cycle of the side chain degradation. The hydratase ChsH1-ChsH2 was identified by Dr. Thomas and Dr. Yang to function for the hydration step at the third cycle of the metabolism (17). The gene of the hydratase ChsH1-ChsH2 is regulated by KstR1 that is same regulon as *rv3538* and *echA19*.

1) Enoyl-CoA hydratases of KstR1 regulon

Rv3538, *echA19*, and *chsH1-chsH2* are the genes of the enoyl-CoA hydratases that are members of the same regulon of KstR1. The enzymes of Rv3538, EchA19, and ChsH1-ChsH2 are candidates for the hydration in the three cycles. Dr. Yang demonstrated that ChsH1-ChsH2 catalyzes the hydration of a steroid enoyl-CoA in the third cycle of cholesterol side chain degradation (17). *Rv3538* is under control by same regulon KstR1, and Rv3538 shares same super family of hot-dogs fold with ChsH1-ChsH2 base on a protein sequence BLAST search. EchA19 is a member of crotonase-like superfamily, but its expression is controlled by same regulon of KstR1 as the expression of ChsH1-ChsH2 and Rv3538. Therefore, Rv3538, EchA19 are predicted to catalyze steroid metabolism similar to the hydration step of ChsH1-ChsH2.

2) Enoyl-CoA hydratases of Mce3R regulon

Mce3R is also known to regulate the expression of the hydratase EchA13 based on the annotation (18). Figure 5 represents the predicted hydration of trans-dodec-2-enoyl-CoA (C12-enoyl-CoA) with EchA13.

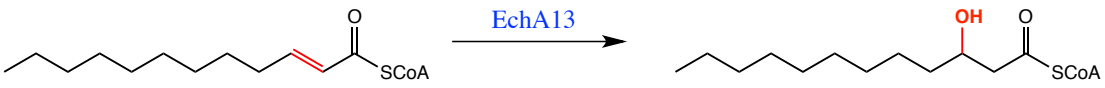

Figure 5 The expected reaction of cholesterol side chain degradation with EchA13

As shown in figure 6, EchA13 is controlled in the same operon as fadE17 and fadE18. The operon is up-regulated by cholesterol and under control by transcriptional regulator Mce3R.

1 operon in the Mce3R regulon

Figure 6 The organization genes of the hydratase, *echA13* gene in the operon

It is possible that the product of the enzymatic reaction with FadE17-FadE18 is the substrate of EchA13 since they are adjacent in a single operon. The expression of FadE17-FadE18 has not been successively completed. As the function of EchA13 is determined, it will help to understand the function of Fad17-FadE18 in cholesterol metabolism of *Mtb*.

Chapter 2. Experiments and methods

2-1. Preparation of materials

Kanamycin, IPTG, and kanamycin plate

The antibiotic kanamycin (30 mg) was dissolved in 1 mL distilled water. The solution of 200 mg of isopropyl β-D-1-thiogalactopyranoside (IPTG) was prepared in 1 mL distilled water. The autoclaved solution of Luria-Bertani (LB) medium (25 g) and agar (15 g) in 1000 mL water were placed on a plate with antibiotic kanamycin (30 μg/ml).

2 × yeast extract trypsin broth (2×YT) and LB medium

A 1 L solution of tryptone (16 g), yeast extract (10 g), and NaCl (5 g) were autoclaved to prepare 2×YT. LB medium for growing the bacterial solution was also autoclaved. The mixture of 10 g of tryptone, 5 g of yeast extract, and 10 g of NaCl was dissolved in 1000 ml of deionized water.

Agarose gel and SDS PAGE gel

Agarose gel was prepared with a heated solution of 100 ml of 0.5 M tris-acetate EDTA (pH 8.0) (TAE) and 1 g of agarose with ethidium bromide (0.2 μg/ml).

Running gel and stacking gel were added into space between glass plates to prepare for

15% SDS PAGE gel. The solution of running gel and stacking gel were prepared by protogel, running buffer, stacking buffer, 10% sulfate polyacrylamide (SDS), 10% ammonium persulfate (APS), and tetramethylenediamine (TEMD).

Preparation of buffers

A binding buffer was prepared with the final concentration of the 920 mM Tris, 0.5 M NaCl, 20 mM imidazole, and 1 mM tris-2-carboxyethylphosphine (TCEP). The pH of the binding buffer was adjusted to pH 8. Elution buffer was prepared with 20 mM Tris, 0.5 M NaCl, 0.25 M imidazole, and 1 mM TCEP. The pH of the elution buffer was pH 8. Desalting buffer was prepared with 50 mM Tris-HCl, 200 mM NaCl, and 1 mM TCEP. The pH of the desalting buffer was confirmed to equal pH 8 before it was used for dialysis.

Preparation of His-tagged gravity column and DHB matrix

The histidine-tagged gravity column was prepared by adding stripping buffer (20 mM Tris HCl, 100 nM EDTA, and 0.5 M NaCl) and 50 mM of $NiSO_4$ onto the gravity column. The matrix substance, 2,5-dihydroxybenzoic acid (DHB), for matrix assisted laser desorption/ionization (MALDI-TOF) mass spectra was prepared with 140 mg of DHB dissolved in 4.9 ml of 0.1% trifluoroacetic acid (TFA) and 2.1 ml of acetonitrile (ACN).

2-2. The general methods to express enoyl-CoA hydratase

Polymerase chain reaction (PCR)

Forward and reverse primer was designed based on the DNA sequence of enoyl-CoA hydratase. The reverse primer was designed based on the sequences of H37Rv strain of *Mtb*. Restriction site sequence of Hind*III* was added to the reverse primer. The melting temperature (Tm) was 75 °C. The forward primer of *echA13* was provided by Dr. Wipperman. In 50 μL reaction volume, 20% GC buffer, 20% DNA of H37Rv strain, 10% each of two diluted primers, 3% dimethyl sulfoxide (DMSO), 2% deoxynucleotide (dNTP), and 1% DNA polymerase were prepared in the PCR tube. The target gene was separated by gel electrophoresis. The PCR product was extracted using QIA quick spin column from the agarose gel.

Preparation of cut pET 28b

The genetic product of pET 28b was transformed into a XL I blue cells. One colony of pET 28b and XL1 blue cell was incubated in 10 mL of LB medium with kanamycin overnight. After a minipreparation of the sample, the DNA product of the pET 28b (74 ng/μl) was cut with restriction enzyme of Nde*I* and Hind*III*. The sample was incubated at 37 °C for 6 hours, and the 60 μL cut pET 28b was purified by ethanol precipitation.

Ligation of the PCR product with cut pET 28b

The restriction enzymes of 4% Hind *III* and Nde*I* were added to 30 μL of the PCR product with 25% buffer 2 nEB. The prepared sample was incubated at 37 °C for 6 hours. After

the PCR product was cut, 2 µL of cut pET 28b, 1 µL T4 ligase buffer, 1 µL of T4 ligase were added to the DNA insertion of the PCR product and incubated at 16 °C for 12 hours. After the incubation, the ligated plasmid was analyzed using gel electrophoresis.

Amplification of the plasmid of enoyl-CoA hydratase and pET 28b

The ligated plasmid of enoyl-CoA hydratase and pET28b was transferred to *Escherichia coli*, XL I blue. LB medium, 1000 µL, was added into the transferred solution and incubated at 37 °C for an hour. The LB medium was autoclaved. The incubated solution was applied on the kanamycin (30 µg/ml) selective agar plate and incubated at 37 °C overnight. One colony and 2.5 µL of kanamycin (100 mg/ml), were added to 5 mL of LB medium, and incubated at 37 °C for 12 hours. The amplified plasmid was purified by minipreparation.

Expression of enoyl-CoA hydratase

1 µM of plasmid (127~µg/ul) was transferred to BL21 (DE3) cell (100 µl). LB medium, 1000 µl, was added to solution of plasmid and BL21 (DE3) cell and incubated at 37 °C for an hour. The 200 µl solution was applied to the kanamycin (30 µg/ml) selective agar plate and incubated at 37 °C for 16 hours.

A single colony of enoyl-CoA hydratase and BL21 (DE3) cells were incubated in 10 mL of LB medium and kanamycin at 37 °C overnight. The induced bacterial solution was incubated in 1L of 2×YT medium with 1000 µL of kanamycin (30 mg/ml). The prepared solution was incubated at 37 °C at 250 rpm for about three hours. When the optical density (OD) of the

incubated solution reached to a value between 0.6-0.8, isopropyl β-D-1-thiogalactopyranoside (IPTG) (400 μmol/ml) was added into the flask. The bacterial solution was incubated at 18 °C overnight. The incubated solution was centrifuged at 6000 rpm speed for 10 minutes. The supernatant was discarded, and ~15 g of cell pellet was stored at -20 °C.

Purification of enoyl-CoA hydratase

The bacterial cells were lysed at 27 kspi using Constant Systems Limited TS-Series cell disruptor. The lysed cells were centrifuged at 40,000 rpm and 4 °C for an hour. The collected supernatant was added to the gravity column. The column was prepared with Ni-NTA agarose. Target protein in about 30 mL supernatant was bound to Ni-NTA column and purified by adding 20 mL eluting buffer into the column.

The purified protein was transferred into a dialysis tube (3500 molecular weight cut-off (MWCO)). The prepared dialysis tube was placed in desalting buffer at 4 °C overnight. The purified protein was analyzed using SDS PAGE gel electrophoresis.

2-3. Rv3538 enoyl-CoA hydratase

Rv3538 was expressed during the research period of undergraduate year. Rv3538 (0.1 μM) was added to 12 μM unsaturated 3-oxo-chol-4-en-24-oyl-CoA (3-OCO-CoA). The unsaturated 3-OCO-CoA was provided by Dr. Lu. The reaction buffer 100 mM 4-(2-hydroxyethyl)-1-piperazineethanesulfonic acid (HEPES) was used, and the enzymatic reaction was incubated at 25 °C. The control reaction without Rv3538 was also monitored. The control and enzymatic reaction product were observed by MALDI-TOF mass spectra. The mass spectrum was acquired using Brucker Autoflex II MALDI-TOF/TOF and analyzed by Flex-Analysis software (Brucker).

The enzymatic and control reaction of 3-OCO-CoA and EchA19 were monitored using MALDI TOF mass spectra. EchA19 (1 μM) was added to the unsaturated 3-OCO-CoA (25 μM). The enzymatic reaction was incubated at 25 °C for 40 minutes. The control and enzymatic reaction product were observed using MALDI TOF mass spectra.

The reaction of 3-OCO-CoA and EchA13 was monitored by MALDI TOF mass spectra. The enzymatic reaction of EchA13 (1 μM) and 3-OCO-CoA (25 μM) was incubated at 25 °C for 40 minutes with 100 mM HEPES buffer in 300 μl reaction volume. The reaction product was observed using MALDI TOF mass spectra. The control reaction without enzyme was also monitored by MALDI TOF mass spectra.

2-4. EchA13 catalyzes hydration of the C12-enoyl-CoA

The total reaction volume was 300 μL, and 100 mM HEPES buffer was used. The substrate of the unsaturated C12-enoyl-CoA was provided by Dr. Lu. EchA13 (1 μM) was added to the 25 μM C12-enoyl-CoA. The reaction was incubated at 25 °C for 40 minutes and monitored by MALDI TOF mass spectra. The 10 μL of the reaction mixture was concentrated using zip-tip before the sample was spotted on the MALDI TOF plate, and the sample was eluted with 1 μl of 0.1% TFA in ACN-H_2O (50%). The ratio of the sample to DHB matrix was 1:1.

After the reaction of C12-enoyl-CoA with EchA13, 25 μM of C12-enoyl-CoA was added to the reaction product. The sample was monitored by MALDI-TOF mass spectra after adding 25 μM of C12-enoyl-CoA. The reaction was incubated at 25 °C for 40 minutes, and the reaction product was observed again by MALDI-TOF mass spectra. Table 3 shows the summary of the samples and the concentrations that were used.

	HEPES	EchA13	C12-enoyl-CoA	H_2O	Incubation Time
1st reaction	100 mM	1 μM	25 μM	138 μL	40 mins
2nd reaction			Adding 25 μM of C12-enoyl-CoA to the 1st reaction	-	40 mins
Control	100 mM	-	25 μM	173 μL	40 mins

Table 3 The reactions of C12-enoyl-CoA and EchA13

The enzymatic reaction of EchA19 and C12-enoyl-CoA was also observed. EchA19 (1 μM) was added to the unsaturated C12-enoyl-CoA (25 μM). The reaction buffer of 100 mM HEPES was used in the 300 μL reaction volume. The enzymatic reaction was incubated at 25 °C for 40 minutes. The reaction product was observed using MALDI TOF mass spectra. The control reaction without enzyme was also observed.

2-5. EchA19 catalyzes hydration of the 3-OCS-CoA cholesterol intermediate

The control reaction of 25 μM saturated 3-OCS-CoA was observed without EchA19 using MALDI TOF mass spectra. The substrate of the saturated 3-OCS-CoA was provided by Dr. Lu.

The dehydrogenase of ChsE4-ChsE5 (1 μM) was added to the 25 μM of the saturated substrate, 3-OCS-CoA. Ferrocenium hexafluorophosphate (250 μM) was added with 100 mM HEPES in the reaction volume of 300 μL. After the reaction was incubated at 25 °C for 40 minutes, the 1st reaction product was observed by MALDI-TOF mass spectra.

The 1 μM of echA19 was added to the 1st reaction product of 3-OCS-CoA and ChsE4-ChsE5 in the reaction volume of 300 μL. The reaction was incubated at 25 °C for 40 minutes. The product of the 2nd reaction was observed by MALDI TOF mass spectra. Zip-tip was used to concentrate the 300 μL enzymatic reaction product, and DHB matrix was used to load the sample on the MALDI TOF plate. The sample in zip-tip was eluted by 1 μl of 0.1% TFA in ACN-H_2O (50%), and the ratio of the sample to DHB matrix was 1:1.

	HEPES	Enzyme	3-OCS-CoA	H_2O	Incubation Time
1st Reaction	100 mM	Adding 1 μM of ChsE4-ChsE5	25 μM	208 μL	40 mins
2nd Reaction	-	Adding 1 μM of EchA19 to the 1st Reaction product	-	-	40 mins
Control	100 mM	-	25 μM	237 μL	40 mins

Table 4 The reactions of 3-OCS-CoA of cholesterol intermediate and EchA19

Table 4 illustrates the samples and their concentrations that were used in the 1st and 2nd reactions. The 1st reaction refers the reaction of 3-OCS-CoA and ChsE4-ChsE5, and the 2nd reaction is the reaction of the product of the 1st reaction and EchA19.

Chapter 3. Results and discussions

3-1. Expression and Purification of the hydratases

Polymerase chain reaction (PCR) for *rv3538* and *echA13*

The reverse primer was designed based on DNA sequences of gene from the H37Rv strain of *Mycobacterium tuberculosis (Mtb)*. Table 5 illustrates the primers of *echA13* and *rv3538* that were designed. The forward primer of *echA13* was obtained from Dr. Wipperman.

Rv3538 Forward primer 5'-TATTATCATATGCCCATCGACTTGGACGTCGCGCTGGGT-3'

Rv3538 Reverse primer 3'-ATAATAAAGCTTCTATGCCGGCACCAGCTCCACTCCGC-3'

EchA13 Reverse primer 5'- ATATATAAGCTTTCAGGGCCGCTGCTTGATCGCG – 3'

Rv number	gene name	vector	His_6 tag	*selection*
Rv3538	*Hsd4B*	*pET28b*	*N-terminal*	*kanamycin*
Rv1935c	*EchA13*	*pET28b*	*N-terminal*	*kanamycin*

Table 5 Gene construct used for the primers (See appendix table A-1 and A-2.)

Ligation of the PCR product with cut pET 28b for *rv3538* and *echA13*

The plasmid of the ligated *echA13* product and cut pET 28b was amplified. The ligated product of the *echA13* insertion and cut pET 28b was confirmed using agarose gel electrophoresis. The DNA band on the agarose gel appeared at 6251 bp. The DNA band was corresponded to the sum of the DNA size of *echA13* (957 bp) and cut pET 28b (5304 bp). Therefore, the ligated product was confirmed to be a plasmid of *echA13* and cut pET 28b. The plasmid of *rv3538* was also analyzed by agarose gel. The DNA band was matched to the correct size of *rv3538* and cut pET28b (861 bp).

Expression and Purification of enoyl-CoA hydratase, EchA13 and Rv3538

The plasmid of *echA13* and pET 28b was transferred to the E. coli (BL21 DE3), and the target protein was expressed. The expressed EchA13 was purified using histidine-tagged gravity column from the bacterial solution of E. coli. The SDS PAGE gel electrophoresis was performed to confirm the purity of EchA13.

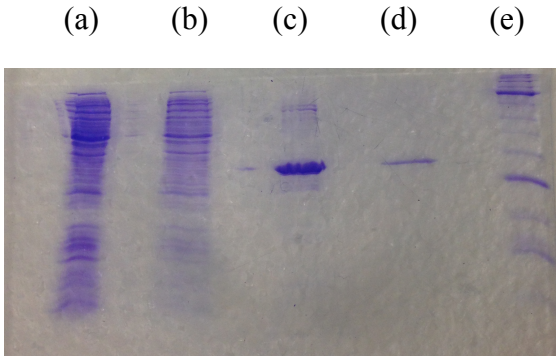

Figure 7 SDS-PAGE gel of EchA13: (a): sample flow; (b): binding buffer; (c): elution buffer; (d): elution buffer; (e): protein ladder

The figure 7 shows the SDS PAGE gel of EchA13. The molecular mass of EchA13 is 35.25 kDa from the annotation of the enzyme. However, the protein band of the purified product with elution buffer was shown at about 28 kDa. The difference could have resulted from the protein ladder because pre-stained ladder is not very accurate.

Rv3538 was also expressed by same protocol as EchA13. Figure 8 represents the SDS PAGE gel of the expressed Rv3538 after His-tag purification. The molecular mass of the expressed Rv3538 was matched with 30.21 kDa.

(a) (b) (c) (d)

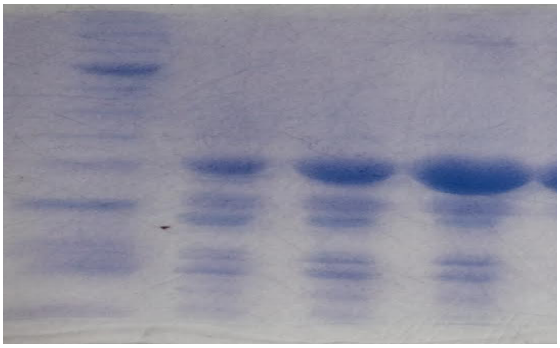

Figure 8 SDS-PAGE gel of Rv3538: (a): protein ladder; (b)-(d): expressed Rv3538

Expression and purification of EchA19, enoyl-CoA hydratase

The plasmid of *echA19* was obtained from Dr. Nesbitt. The plasmid of *echA19* was transferred to E. coli (BL 21 DE3). The bacterial sample was amplified in 1 L of 2XY medium with kanamycin, and ~ 5 g cell pellet was produced. The target protein of EchA19 was purified using histidine-tagged gravity column. Figure 9 shows the SDS PAGE gel of the purified EchA19. The protein band was shown around 28 kD on the SDS PAGE gel, which was the correct band size of 28.248 kD from the annotation. The concentration of EchA19 was measured by UV spectroscopy at 280 nm. The extinction coefficient of EchA19 was 17210 $M^{-1}cm^{-1}$, and the concentration of the purified EchA19 was measured as 59.9 mM.

(a) (b) (c)

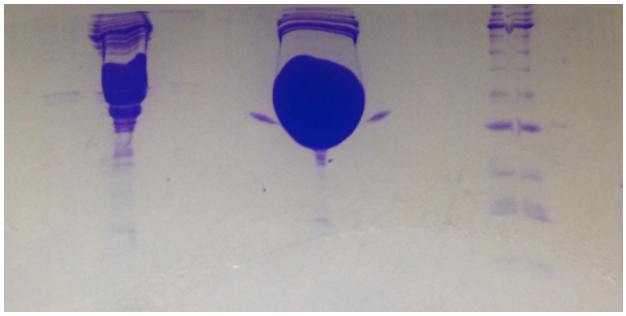

Figure 9 The SDS PAGE gel of EchA19: (a): the sample of old EchA19; (b): the freshly purified EchA19; (c): protein ladder

3-2. Rv3538 enoyl-CoA hydratase with 3-OCO-CoA

The reaction of Rv3538 and unsaturated 3-oxo-chol-4-en-24-oyl-CoA (3-OCO-CoA) was monitored using MALDI-TOF mass spectra. Figure 10 shows the MALDI-TOF mass spectrum of the control reaction of unsaturated 3-OCO-CoA (12 μM) without enzyme. As shown in figure 10, the peak of the starting material of the unsaturated 3-OCO-CoA was observed at 1118 m/z.

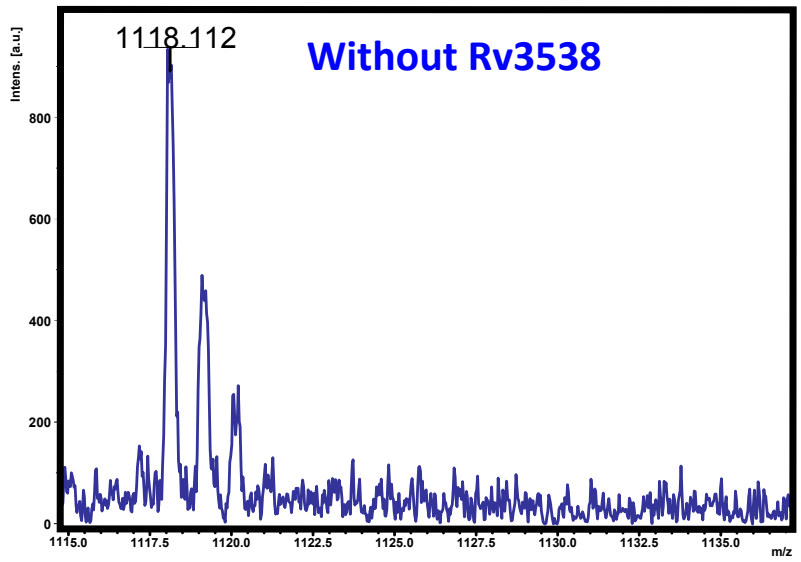

Figure 10 MALDI-TOF mass spectrum of the control reaction of unsaturated 3-OCO-CoA (12 μM) without Rv3538 (See appendix figure A-1 for full spectrum).

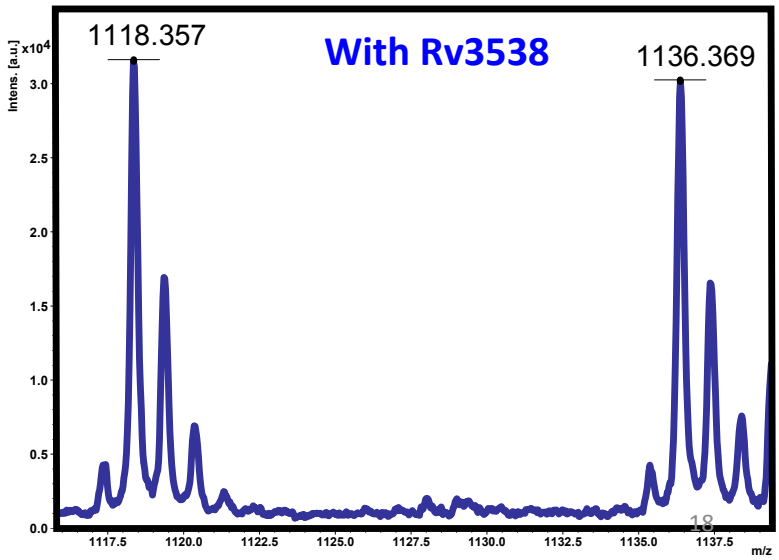

Figure 11 MALDI TOF mass spectrum of the enzymatic reaction product of Rv3538 and unsaturated 3-OCO-CoA (See appendix figure A-2 for full spectrum).

Figure 11 represents the MALDI TOF mass spectrum of the enzymatic reaction of Rv3538 and unsaturated 3-OCO-CoA. As shown in figure 11, hydrated product of the enzymatic

reaction was observed for the peak at 1136 m/z. The difference in mass (m/z) between 1118 and 1136 m/z is 18 m/z, which is the molecular mass of H_2O. The product of the hydrated substrate was confirmed by increase in molecular mass of the substrate by 18 m/z, the molecular mass of H_2O, a fragment produced from the product. As a result, Rv3538 functioned as hydratase with cholesterol intermediate substrate, 3-OCO-CoA.

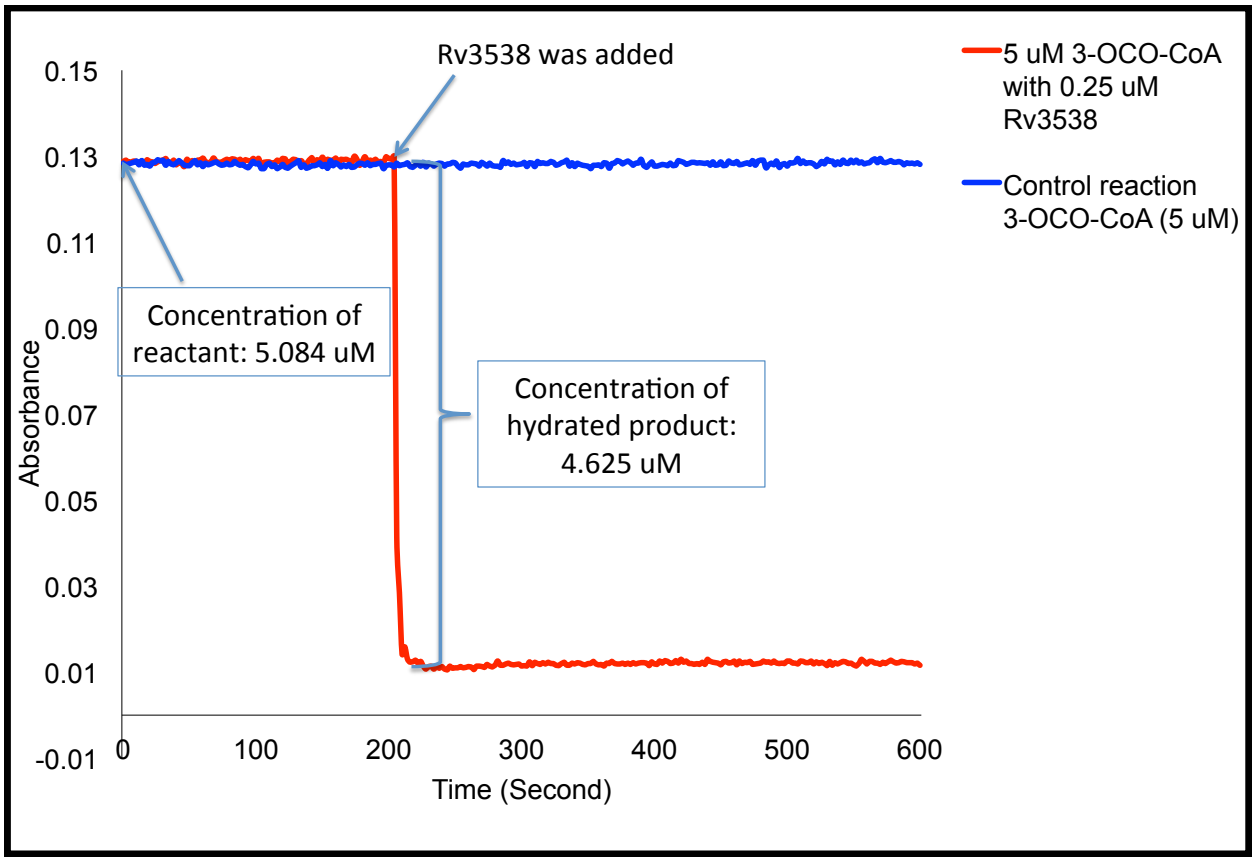

Figure 12 Observation of the reaction of 3-OCO-CoA and Rv3538 by ultraviolet-visible (UV) spectroscopy

The reaction of 5 µM 3-OCO-CoA and 0.25 µM Rv3538 was observed at 263 nm wavelengths by Ultraviolet-visible (UV) spectroscopy. In figure 12, the blue line represents the control reaction, and red line shows enzymatic reaction. Rv3538 was added to the reaction

sample at about 3 minutes. Since the double bond in the side chain is observed at 263 nm wavelengths, hydration is monitored by decrease in absorbance values, which is resulted from disappearing double bond. Therefore, the formation of the hydrated product leads to the decrease in absorbance values. The concentration of the hydrated product was calculated by Beer's law ($A=\varepsilon bc$, where A is absorbance, ε is the extinction coefficient 25336 $M^{-1}cm^{-1}$ at 263 nm, b is the length of the sample and c is the concentration). The concentration of the reactant at starting point was also calculated by Beer's law. As shown in figure 12, the concentration of reactant at 3 minutes was 5.084 μM, and the concentration of hydrated product was 4.625 μM. If the one mole of the reactant would be hydrated to one mole of the product, the equilibrium constant (K_{eq}) of the reaction would be 0.910 M^{-1}. It means that 53 % reactant and 47 % product would be in the reaction sample when the reaction reaches to the equilibrium state. Since the composition of the final product does not change by enzyme or substrate concentration, the enzymatic reaction result of UV spectroscopy was compared to the result of MALDI TOF mass spectrum. Both experiments show the composition of 53 % unsaturated side chain substrate and 47 % hydrated side chain product. Therefore, the reactions reached at same equilibrium state, and K_{eq} of the reaction could be 0.910 M^{-1} at 25 °C.

The enzymatic reactions of EchA13 and EchA19 with unsaturated 3-OCO-CoA were also monitored using MALDI-TOF mass spectroscopy.

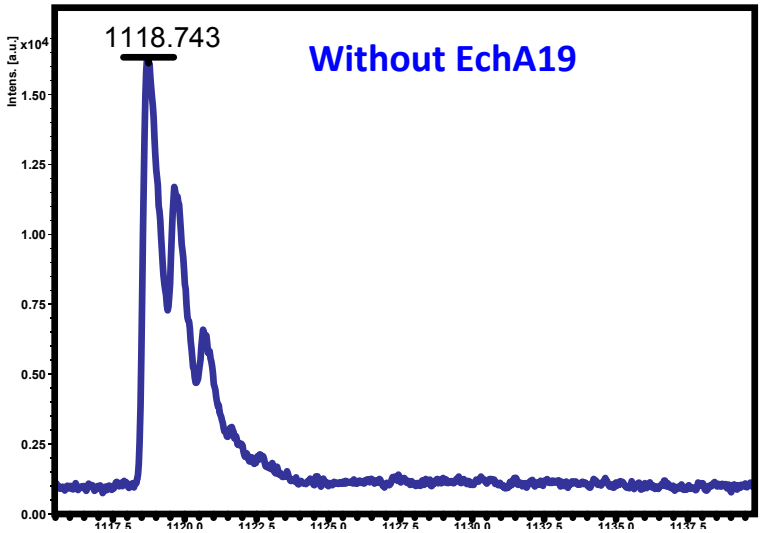

Figure 13 MALDI TOF mass spectrum of the control reaction of unsaturated 3-OCO-CoA (25 µM) without EchA19 (See appendix figure A-3 for full spectrum).

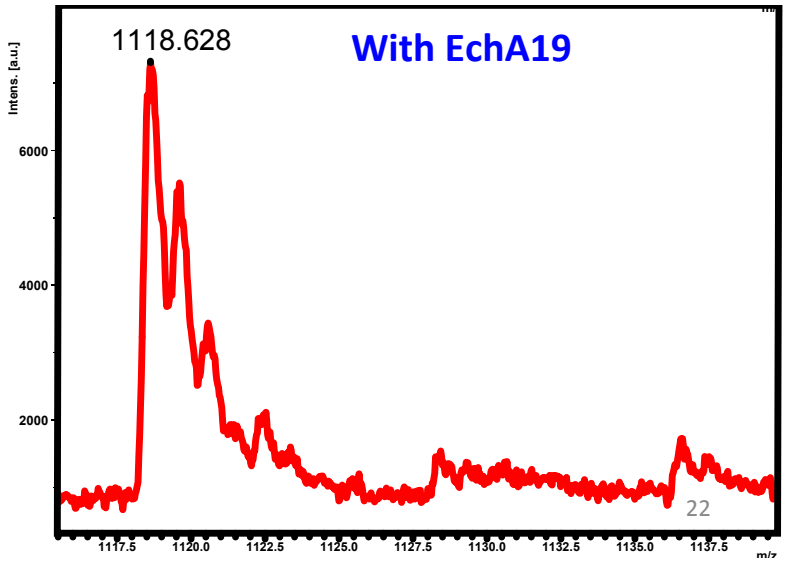

Figure 14 MALDI TOF mass spectrum of the enzymatic reaction product of EchA19 (1 µM) and unsaturated 3-OCO-CoA (25 µM) (See appendix figure A-4 for full spectrum).

Figure 13 represents the control reaction that contains only the unsaturated substrate of 3-OCO-CoA without enzyme. Figure 14 shows the MALDI TOF mass spectrum of the reaction product of EchA19 and unsaturated 3-OCO-CoA. The peak at 1118 m/z represents the starting material of the unsaturated 3-OCO-CoA (25 µM). If EchA19 hydrates the substrate, the hydrated

product would be observed at 1136 m/z. However, as shown in figure 14, the hydrated product was not observed after the reaction was incubated with EchA19. Therefore, EchA19 did not function as a hydratase with unsaturated 3-OCO-CoA or the enzymatic reaction very slowly progressed.

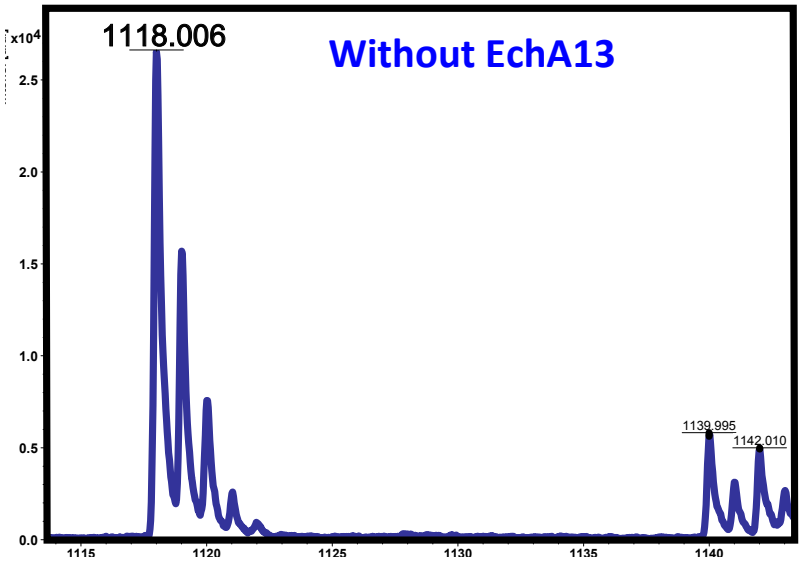

Figure 15 MALDI TOF mass spectrum of the control reaction of the unsaturated 3OCO-CoA (25 µM) without EchA13 (See appendix figure A-5 for full spectrum).

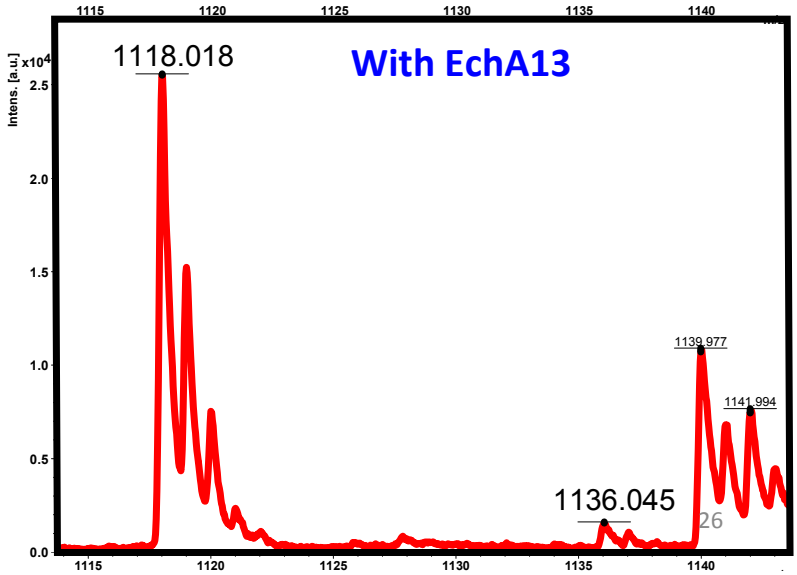

Figure 16 MALDI TOF mass spectrum of the enzymatic reaction of EchA13 (1 µM) and the unsaturated 3-OCO-CoA (25 µM) (See appendix figure A-6 for full spectrum).

Figure 15 shows the control reaction without EchA13 and figure 16 represents the enzymatic reaction of EchA13 (1 μM) and the unsaturated 3-OCO-CoA (25 μM). On the figure 15, the peak at 1118 m/z represents the starting material of unsaturated 3-OCO-CoA, and the peak at 766 m/z shows the CoAs. As shown in the figure 16, the peak at 1136 m/z, the hydrated 3-OCO-CoA was not observed. Therefore, EchA13 did not function as a hydratase for the unsaturated 3-OCO-CoA or the reaction was very slow.

3-3. EchA13 catalyzes hydration of the C12-enoyl-CoA

MALDI TOF mass spectrum of EchA13 with C12-enoyl-CoA

The reaction of EchA13 and trans-dodec-2-enoyl-CoA (C12-enoyl-CoA) was performed to determine the activity of EchA13 with C12-enoyl-CoA. The hydration was confirmed by formation of the hydrated product. Figure 17 illustrates the steps used to determine whether EchA13 hydrates C12-enoyl-CoA or not.

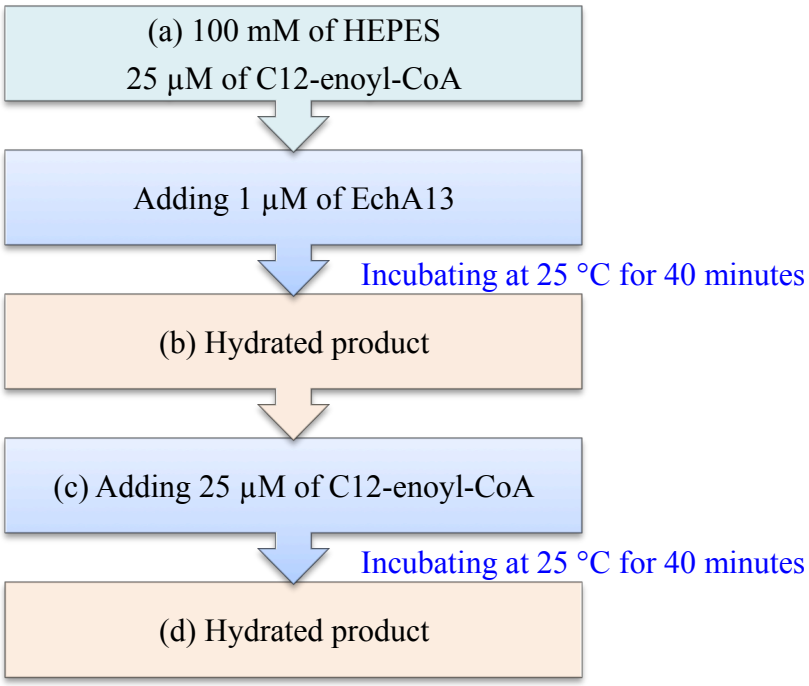

Figure 17 The experiment to test the activity of EchA13 with the substrate C12-enoyl-CoA: the sample of (a), (b), (c), and (d) were analyzed by MALDI TOF mass spectra.

As shown in figure 18, the starting material of C12-enoyl-CoA contained both of the unsaturated and hydrated substrate. Therefore, the activity of the hydratase was determined by the difference of the ratio for the peak intensities of the unsaturated and the hydrated of C12-enoyl-CoA. MALDI TOF mass spectrum was used to observe the reaction product.

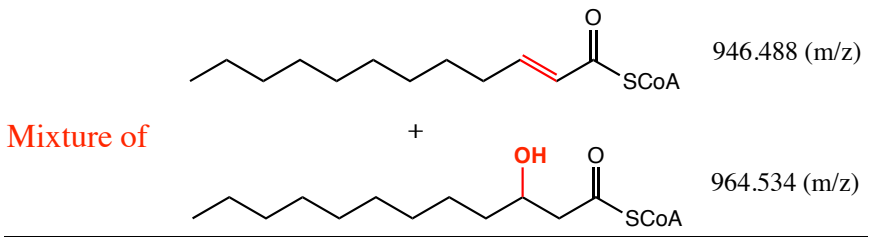

Figure 18 The starting material of the mixture of the unsaturated and hydrated C12-enoyl-CoA

The ratio of unsaturated to hydrated C12-enoyl-CoA was 1:1 in the starting material of C12-enoyl-CoA (25 μM). Figure 19 represents the MALDI TOF mass spectrum of the starting material of C12-enoyl-CoA as a control reaction.

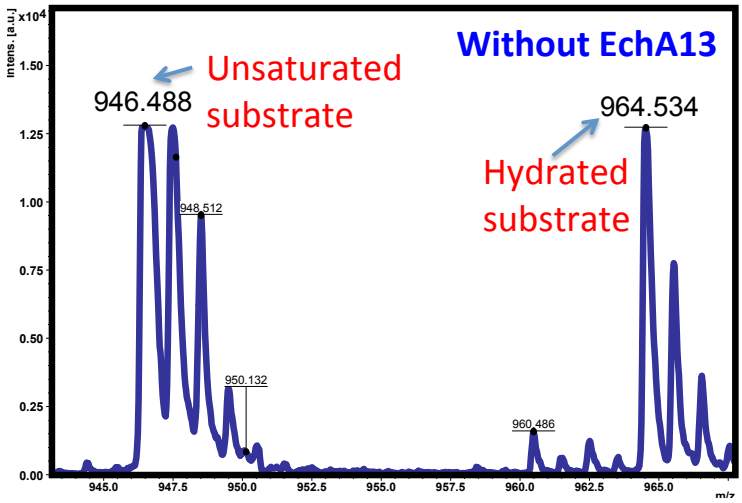

Figure 19 The MALDI TOF mass spectrum for the starting material of 25 μM C12-enoyl-CoA (See appendix figure A-7 for full spectrum).

On the figure 19, the peak of 946.488 m/z represents the unsaturated C12-enoyl-CoA. The peak of 964.534 m/z shows the hydrated C12-enoyl-CoA. The ratio of the intensities of those peaks is 1. After analyzing the starting material, EchA13 (1 μM), was added to the 25 μM of C12-enoyl-CoA as shown in the figure 20.

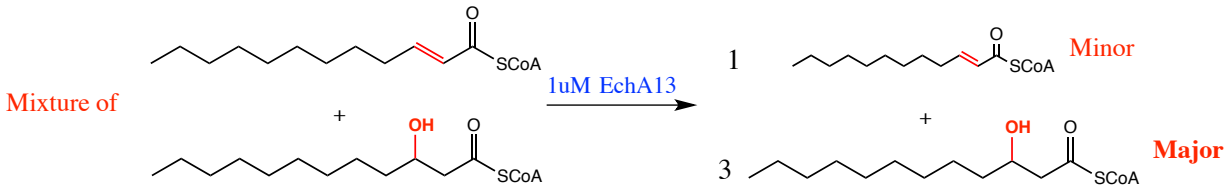

Figure 20 The enzymatic reaction of C12-enoyl-CoA and hydratase candidate of EchA13

Figure 20 demonstrates the reaction of C12-enoyl-CoA and EchA13 (1 µM). The reaction sample was incubated at 25 °C for 40 minutes. The reaction product was analyzed by MALDI TOF mass spectrum. The ratio of unsaturated to hydrated C12-enoyl-CoA changed to 1:3 from 1:1 after incubating with EchA13. Figure 21 shows the MALDI TOF mass spectrum of the reaction product of C12-enoyl-CoA and EchA13.

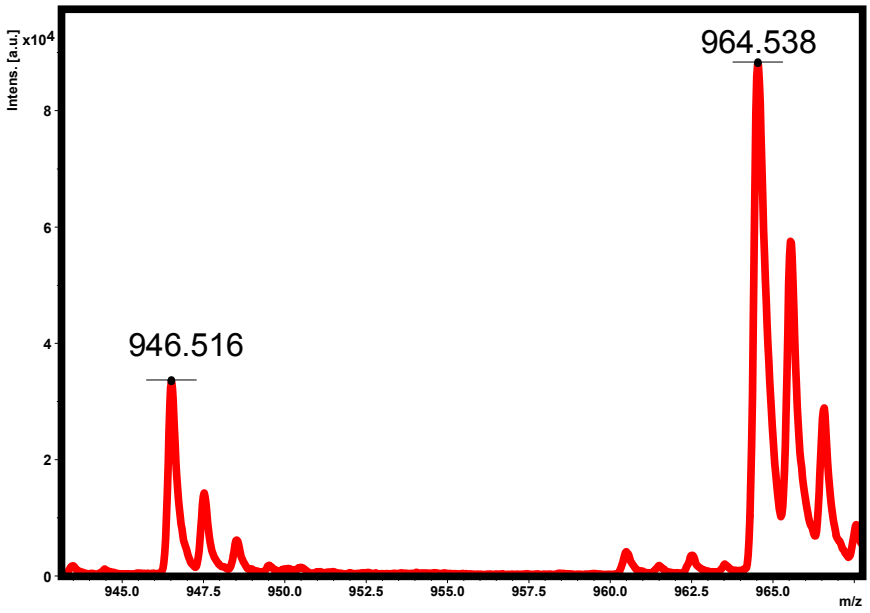

Figure 21 The enzymatic reaction of C12-enoyl-CoA (25 µM) and EchA13 (1 µM): The hydrated product became a major compound in the mixture of the unsaturated and hydrated C12-enoyl-CoA (See appendix figure A-8 for full spectrum).

On the figure 21, the peak of 946.516 m/z represents the unsaturated C12-enoyl-CoA, and the peak at 964.538 m/z shows the hydrated C12-enoyl-CoA. The difference in mass (m/z) between those peaks is 18 m/z, which is the molecular weight of H_2O. The ratio of the peak intensities at 946.516 m/z to 964.538 m/z was changed from 1:1 to 1:3 after the reaction sample was incubated with EchA13 at 25 °C. Therefore, EchA13 hydrated at the double bond of C12-enoyl-CoA.

As shown in figure 22, the reaction product of C12-enoyl-CoA and EchA13 was used to observe whether EchA13 remaining in the sample was still active or not. If the remaining EchA13 is still active, it proves that the hydration of C12-enoyl-CoA occurred by EchA13. Therefore, 25 μM of C12-enoyl-CoA was added to the remaining EchA13 and the reaction product of the C12-enoyl-CoA and EchA13.

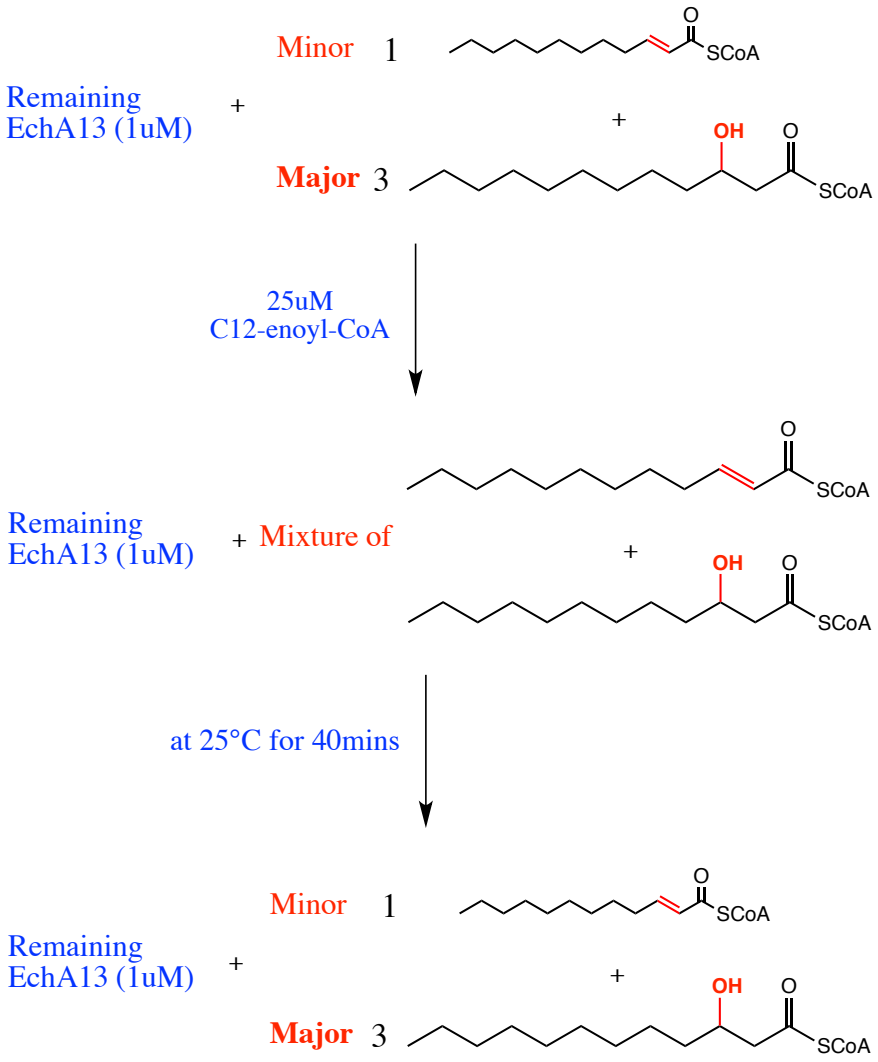

Figure 22 The experiment of reaction product of EchA13 and C12-enoyl-CoA, remaining EchA13 (1 μM), and C12-enoyl-CoA (25 μM)

After 25 µM of C12-enoyl-CoA was added to the remaining EchA13 with the reaction product of EchA13 and C12-enoyl-CoA, the sample was analyzed using MALDI TOF mass spectra before the incubation of the reaction.

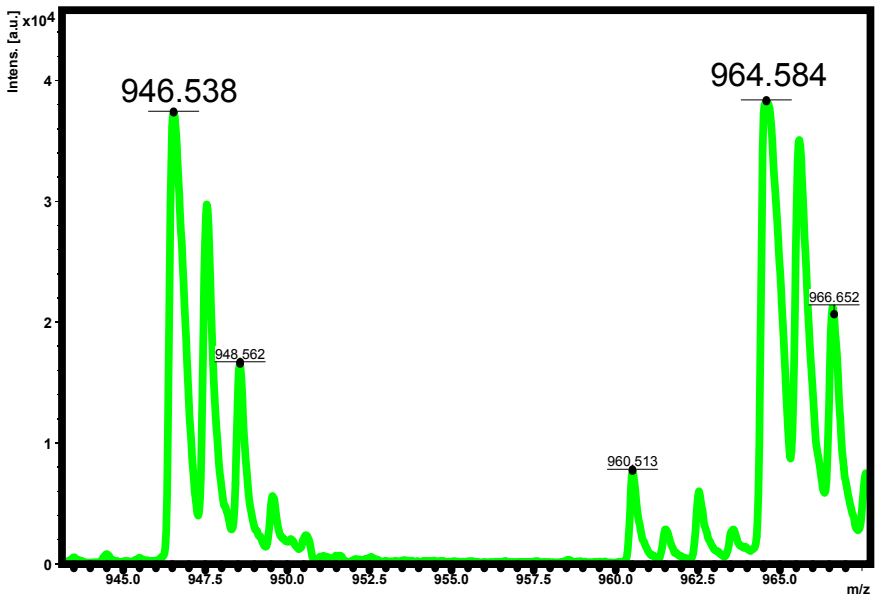

Figure 23 The MALDI TOF mass spectrum of the solution that contains C12-enoyl-CoA (25 µM), the reaction product of C12-enoyl-CoA and EchA13, and the remaining EchA13 before the incubation: The ratio of the peak intensities at 946.538 m/z to 964.584 m/z was 1:1 (See appendix figure A-9 for full spectrum).

On the figure 23, 946.538 m/z represents the peak of unsaturated C12-enoyl-CoA, and the peak of 964.584 m/z shows the hydrated C12-enoyl-CoA. According to the MALDI TOF mass spectra, the ratio of unsaturated to hydrated C12-enoyl-CoA was changed to 1:1 from 1:3 after adding C12-enoyl-CoA to the reaction product. Therefore, the same amount of the unsaturated and the hydrated C12-enoyl-CoA were existed in the sample. The sample was incubated at 25 °C for 40 minutes to allow the enzymatic reaction to be progressed.

The product of the incubated reaction was analyzed by MALDI TOF mass spectrum. After the enzymatic reaction, the ratio of the unsaturated to hydrated C12-enoyl-CoA was changed from 1:1 to 1:3.

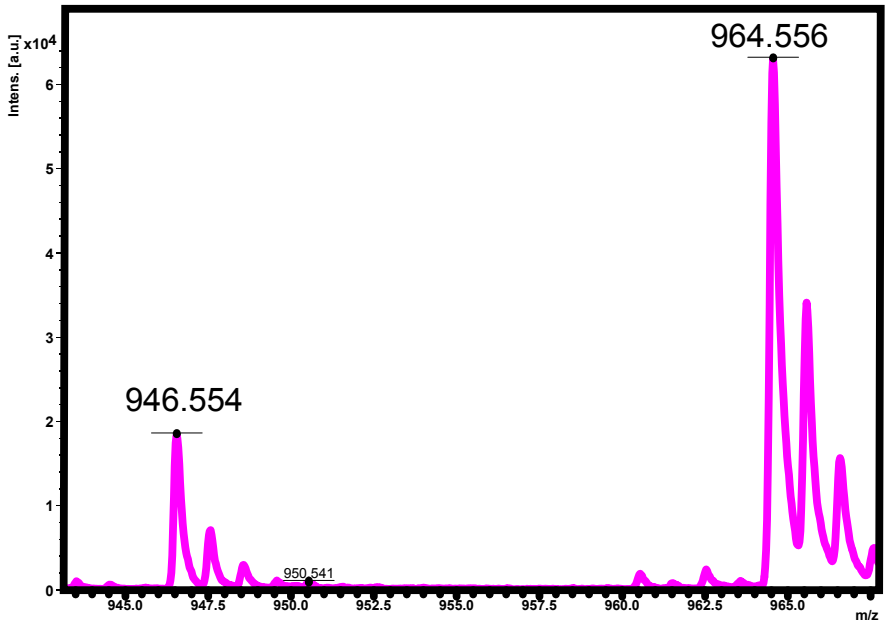

Figure 24 The MALDI TOF mass spectrum of the incubated reaction of the extra C12-enoyl-CoA, the enzymatic reaction product, and the remaining echA13: The ratio of the intensities at 946.554 to 964.556 (m/z) was 1:3 (See appendix figure A-10 for full spectrum).

Figure 24 shows the MALDI TOF mass spectrum that was monitored after the incubation of C12-enoyl-CoA, the enzymatic reaction product, and remaining EchA13 at 25 °C for 40 minutes. The ratio of the intensity at 946.554 m/z for the unsaturated C12-enoyl-CoA to the intensity of 964.556 m/z for the hydrated C12-enoyl-CoA was changed from 1:1 to 1:3. As a result, the hydrated C12-enoyl-CoA became a major component, whereas unsaturated C12-enoly-CoA was a minor compound. Therefore, the remained EchA13 in the reaction was still active. Furthermore, the ratio of unsaturated to hydrated C12-enoyl-CoA was 1:3, which is same

as the ratio in figure 21. Therefore, the equilibrium constant of the reaction could be estimated as 3 M^{-1}.

The enzymatic reaction of EchA19 (1 µM) and C12-enoyl-CoA (25 µM) was monitored using MALDI TOF mass spectra. 1 µM EchA19 was added to the 25µM unsaturated C12-enoyl-CoA, and the reaction was incubated at 25 °C for 40 minutes. The control reaction was also monitored to compare the starting material of C12-enoyl-CoA to the enzymatic reaction product.

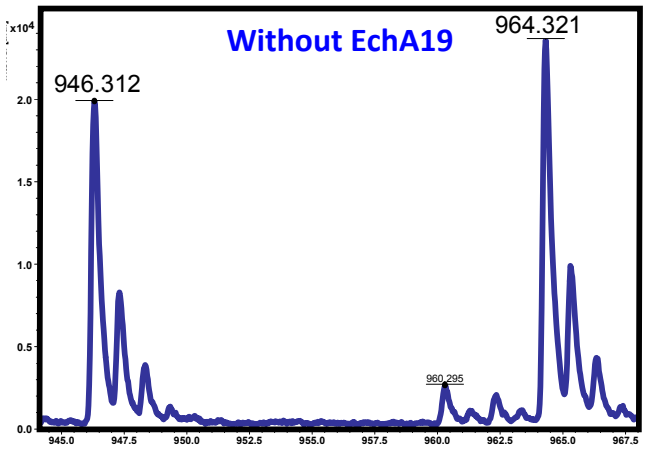

Figure 25 MALDI TOF mass spectrum of the control reaction of C12-enoyl-CoA without EchA19 (See appendix figure A-11 for full spectrum).

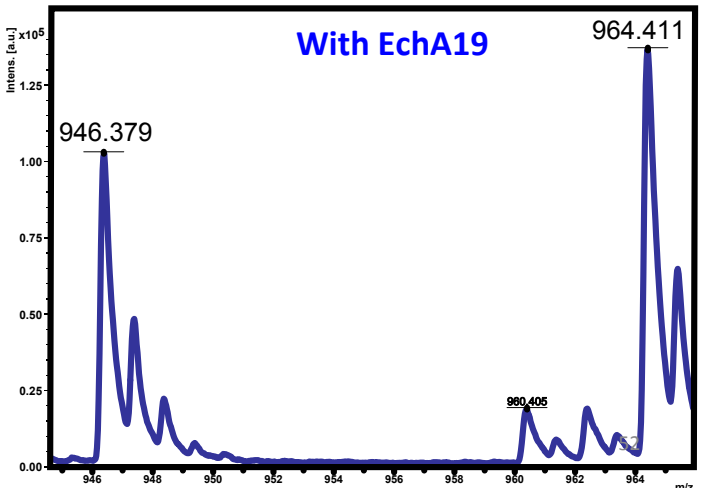

Figure 26 MALDI TOF mass spectrum of the enzymatic reaction of C12-enoyl-CoA (25 µM) and EchA19 (1 µM) (See appendix figure A-12 for full spectrum).

Figure 25 represents the MALDI TOF mass spectrum of the control reaction, and figure 26 shows the MALDI TOF mass spectrum of the enzymatic reaction. On the figure 25 and 26, the peaks at 946 m/z and 964 m/z represent the unsaturated C12-enoyl-CoA and hydrated C12-enoyl-CoA. After the reaction was incubated with EchA19 (1 μM), the ratio of the intensities of two peaks did not change. Therefore, EchA19 did not function as a hydratase with C12-enoyl-CoA.

3-4. EchA19 catalyzes hydration of the 3-OCS-CoA cholesterol intermediate

MALDI TOF mass spectrum of EchA19 with 3-OCS-CoA and ChsE4-ChsE5

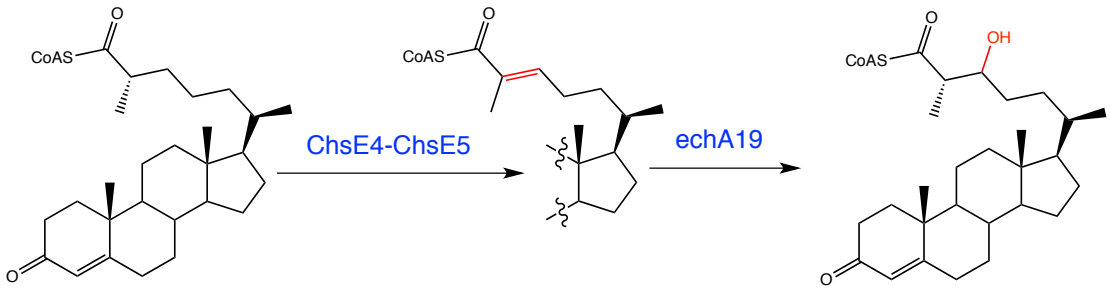

Figure 27 The dehydrogenation and hydration at the 1st cycle of the cholesterol metabolism: 3-OCS-CoA is a substrate of the 1st cycle of the side chain degradation.

The enzymatic reaction of EchA19 and 3-oxo-cholest-4-en-26-oyl-CoA (3-OCS-CoA) of the cholesterol intermediate was observed. Figure 27 shows the dehydrogenation and hydration of the substrate 3-oxo-cholest-4-en-26-oyl-CoA (3-OCS-CoA) with dehydrogenase of ChsE4-ChsE5 and EchA19. 3-OCS-CoA is cholesterol intermediate in the 1st cycle of the side chain degradation, and EchA19 is a hydratase candidate for the hydration of the unsaturated 3-OCS-

CoA. ChsE4-ChsE5 is known as dehydrogenase at the 1st cycle of the metabolism. The dehydrogenation of 3-OCS-CoA with ChsE4-ChsE5, and the reaction of unsaturated 3-OCS-CoA with EchA19 were observed using MALDI TOF mass spectroscopy. Figure 28 represents the experimental process used to test the activity of EchA19 with the substrate of 3-OCS-CoA.

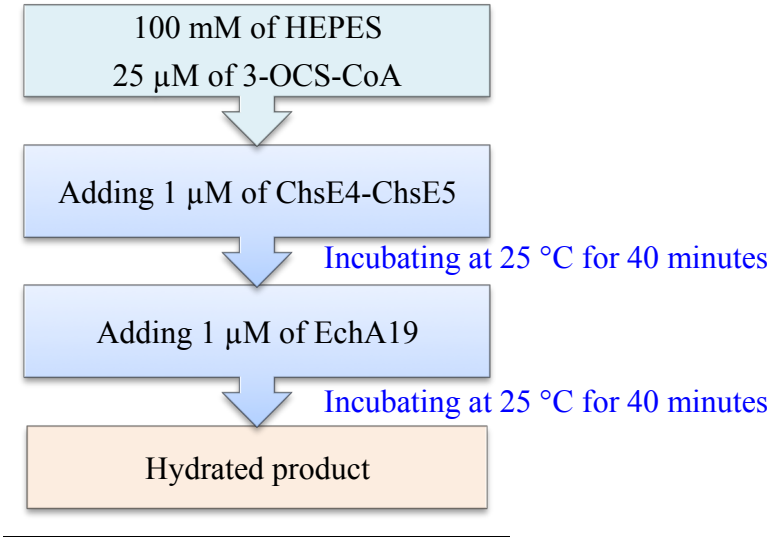

Figure 28 The series of steps performed to determine the activity of EchA19: the saturated 3-OCS-CoA was dehydrogenated by ChsE4-ChsE5, and then the unsaturated 3-OCS-CoA was tested using the hydratase candidate EchA19.

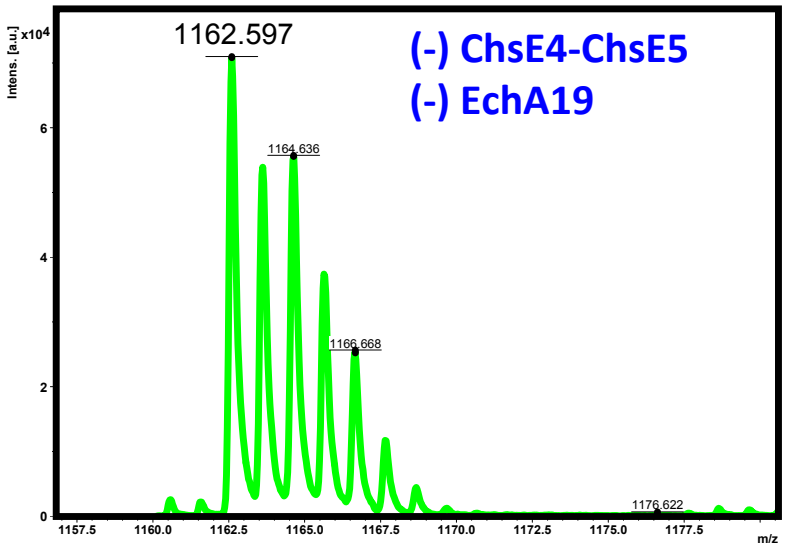

Figure 29 The MALDI TOF mass spectrum of 3-OCS-CoA as a control reaction: the peak at 1162.597 m/z represents the saturated 3-OCS-CoA (See appendix figure A-13 for full spectrum).

The control reaction of 3-OCS-CoA without enzyme was also observed. Figure 29 shows the mass spectrum of the control reaction. Within the figure 29, the peak at 1162.597 m/z represents the saturated 3-OCS-CoA.

The reaction of the saturated 3-OCS-CoA with ChsE4-ChsE5 was observed. The dehydrogenase of ChsE4-ChsE5 (1uM) was added to the 3-OCS-CoA (25uM). The reaction mixture was incubated at 25 °C for 40 minutes. The incubated sample was monitored by MALDI TOF mass spectrum.

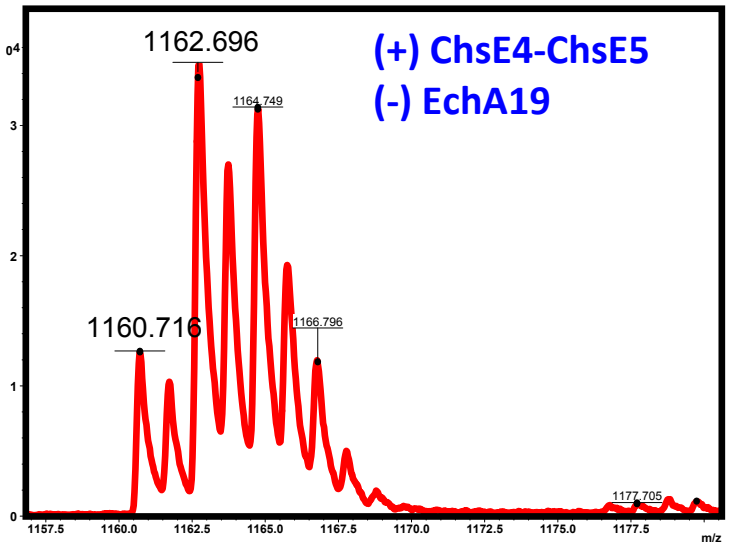

Figure 30 The MALDI TOF mass spectrum of the reaction product of 3-OCS-CoA and ChsE4-ChsE5: The peak of the dehydrogenated 3-OCS-CoA was observed after adding ChsE4-ChsE5 (See appendix figure A-14 for full spectrum).

Figure 30 represents the product from the dehydrogenation of 3-OCS-CoA (25uM) after incubating the sample with ChsE4-ChsE5 (1uM). The peak at 1162.76 m/z represents the saturated 3-OCS-CoA. The peak at 1160.753 m/z is corresponded to the dehydrogenated 3-OCS-CoA. The product of the unsaturated 3-OCS-CoA was analyzed as decrease in mass of 2 m/z on the MALDI TOF mass spectrum. As a result, 3-OCS-CoA was successfully dehydrogenated by ChsE4-ChsE5.

EchA19 (1uM) was added to the reaction product of 3-OCS-CoA and ChsE4-ChsE5. The reaction mixture of the dehydrogenated 3-OCS-CoA and EchA19 was incubated at 25 °C for 40 minutes. The reaction product was analyzed by MALDI TOF mass spectrum to monitor whether the unsaturated 3-OCS-CoA was hydrated by EchA19 or not. Figure 31 represents the MALDI TOF mass spectrum of the reaction product of unsaturated 3-OCS-CoA and EchA19.

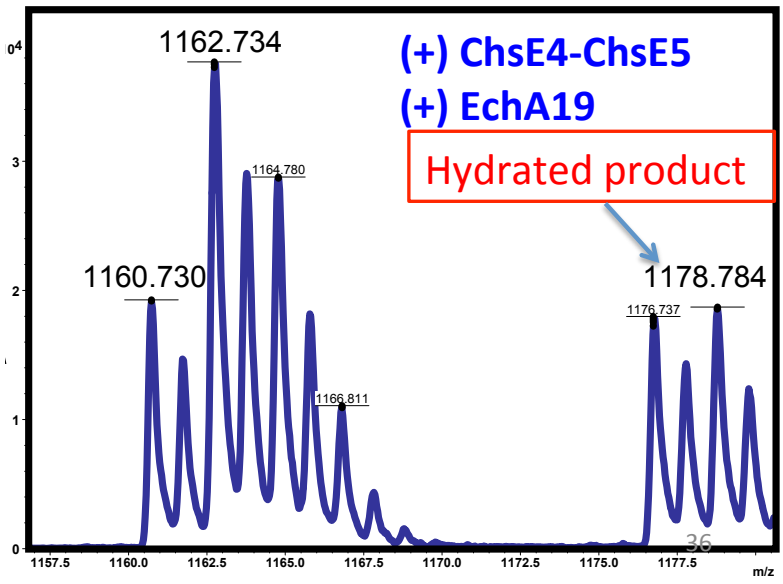

Figure 31 The MALDI TOF mass spectrum of the reaction product of unsaturated 3-OCS-CoA and EchA19: the unsaturated 3-OCS-CoA was hydrated by EchA19 (See appendix figure A-15 for full spectrum).

In Figure 31, the peak at 1162.734 m/z represents the starting material of 3-OCS-CoA, and the peak at 1160.730 m/z represents the unsaturated 3-OCS-CoA produced from the dehydrogenase ChsE4-ChsE5. As shown on the figure 31, the peak at 1178.784 m/z was observed after adding EchA19 to the dehydrogenated 3-OCS-CoA. The difference in mass between the peaks of the dehydrogenated and hydrated 3-OCS-CoA is 18 m/z, which is a molecular weight of H_2O. Therefore, proving the difference in mass between 1160.730 and 1178.784 m/z was 18 m/z. Thus, the hydrated product could be confirmed by increase in mass of 18 m/z. As a result, EchA19 functioned as hydratase with unsaturated 3-OCS-CoA based on the MALDI TOF mass spectrum.

Chapter 4. Conclusion and future directions

4-1. EchA13 catalyzes hydration of the C12-enoyl-CoA

Mce3R regulon controls the enzyme expression of EchA13, FadE17, and FadE18. In this project, EchA13 was expressed and tested with unsaturated trans-dodec-2-enoyl-CoA (C12-enoyl-CoA). As a result, enoyl-CoA hydratase candidate EchA13 hydrated C12-enoyl-CoA. Therefore, EchA13 catalyzes the C12-enoyl-CoA degradation. EchA19 was also expressed and tested with unsaturated C12-enoyl-CoA. However, EchA19 did not function as a hydratase with C12-enoyl-CoA.

Since the expression of EchA13, FadE17 and FadE18 is controlled by same regulon, the product of the enzymatic reaction of C12-enoyl-CoA and EchA13 is expected to be the substrate of FadE17 or FadE18. The investigation of EchA13 would give beneficial information to identify FadE17 and FadE18 in the future experiments.

4-2. EchA19 and Rv3538 catalyzes hydration of the cholesterol intermediate side chain

KstR1 regulon controls the enzyme expression of Rv3538, EchA19, and ChsH1-ChsH2. Since the genes of those enoyl-CoA-hydratases share same regulon of KstR1, they are expected to have similar functions for the cholesterol metabolism. As shown in figure 1, the degradation of the cholesterol side chain consists of three cycles. The 3-oxo-cholest-4-en-26-oyl-CoA (3-OCS-CoA) is substrate of the 1st cycle, and the substrate of the 2nd cycle is 3-oxo-chol-4-en-24-

oyl-CoA (3-OCO-CoA). The enoyl-CoA-hydratase, ChsH1-ChsH2, was identified by Dr. Yang to be a hydratase for the substrate of the 3rd cycle, 3-OPC-CoA.

In this project, Rv3538 was observed to hydrate the unsaturated 3-OCO-CoA of the 2nd cycle of the side chain degradation. However, EchA19 and EchA13 did not function as hydratase for the unsaturated 3-OCO-CoA or the reaction was very slow.

Enoyl-CoA-hydratase EchA19 was also expressed and tested with dehydrogenated 3-OCS-CoA, which is the 1st cycle substrate. As a result, the unsaturated 3-OCS-CoA was hydrated by EchA19. The starting material of the saturated 3-OCS-CoA was analyzed as a control reaction. The peak of unsaturated 3-OCS-CoA was monitored after adding dehydrogenase, ChsE4-ChsE5, to the saturated 3-OCS-CoA. The peak of the hydrated 3-OCS-CoA was also observed after EchA19 was added to the dehydrogenated 3-OCS-CoA. The difference in mass (m/z) between the peaks of unsaturated and hydrated 3-OCS-CoA was 18 m/z, which is a molecular mass of H_2O. Therefore, EchA19 hydrates the 1st cycle substrate 3-OCS-CoA of the cholesterol side chain degradation.

The enoyl-CoA-hydratase, Rv3538 hydrates the 2nd cycle substrate of 3-OCO-CoA. EchA19 catalyzes the hydration for the 1st cycle substrate of 3-OCS-CoA. The experiment to investigate further information about the activity of the hydratase candidates for the cholesterol intermediate needs to be designed for the future work.

References

1. Frieden, T. R., et al. (2003). "Tuberculosis." Lancet **362**(9387): 887-899.
2. Thomas, S. T., et al. (2011). "Inhibition of the M. tuberculosis 3beta-hydroxysteroid dehydrogenase by azasteroids." Bioorg Med Chem Lett **21**(8): 2216-2219.
3. Mueller, P. and J. Pieters (2006). "Modulation of macrophage antimicrobial mechanisms by pathogenic mycobacteria." Immunobiology **211**(6-8): 549-556.
4. Bass, J. B., Jr., et al. (1994). "Treatment of tuberculosis and tuberculosis infection in adults and children. American Thoracic Society and The Centers for Disease Control and Prevention." Am J Respir Crit Care Med **149**(5): 1359-1374.
5. Falzon, D., et al. (2011). "WHO guidelines for the programmatic management of drug-resistant tuberculosis: 2011 update." Eur Respir J **38**(3): 516-528.
6. Gandhi, N. R., et al. (2010). "Multidrug-resistant and extensively drug-resistant tuberculosis: a threat to global control of tuberculosis." Lancet **375**(9728): 1830-1843.
7. Pablos-Mendez, A., et al. (1998). "Global surveillance for antituberculosis-drug resistance, 1994-1997. World Health Organization-International Union against Tuberculosis and Lung Disease Working Group on Anti-Tuberculosis Drug Resistance Surveillance." N Engl J Med **338**(23): 1641-1649.
8. Gandhi, N. R., et al. (2006). "Extensively drug-resistant tuberculosis as a cause of death in patients co-infected with tuberculosis and HIV in a rural area of South Africa." Lancet **368**(9547): 1575-1580.
9. Nguyen, L. and J. Pieters (2005). "The Trojan horse: survival tactics of pathogenic mycobacteria in macrophages." Trends Cell Biol **15**(5): 269-276.

10. Datta, M., et al. (2015). "Anti-vascular endothelial growth factor treatment normalizes tuberculosis granuloma vasculature and improves small molecule delivery." Proceedings of the National Academy of Sciences of the United States of America **112**(6): 1827-1832.
11. Russell, D. G., et al. (2009). "Foamy macrophages and the progression of the human tuberculosis granuloma." Nat Immunol **10**(9): 943-948.
12. Wipperman, M. F., et al. (2014). "Pathogen roid rage: cholesterol utilization by Mycobacterium tuberculosis." Crit Rev Biochem Mol Biol **49**(4): 269-293.
13. Houben, E. N., et al. (2006). "Interaction of pathogenic mycobacteria with the host immune system." Curr Opin Microbiol **9**(1): 76-85.
14. Sundaramurthy, V. and J. Pieters (2007). "Interactions of pathogenic mycobacteria with host macrophages." Microbes Infect **9**(14-15): 1671-1679.
15. Yang, M., et al. (2015). "Unraveling Cholesterol Catabolism in Mycobacterium tuberculosis: ChsE4-ChsE5 alpha2beta2 Acyl-CoA Dehydrogenase Initiates beta-Oxidation of 3-Oxo-cholest-4-en-26-oyl CoA." ACS Infect Dis **1**(2): 110-125.
16. Yang, M., et al. (2014). "A distinct MaoC-like enoyl-CoA hydratase architecture mediates cholesterol catabolism in Mycobacterium tuberculosis." ACS Chem Biol **9**(11): 2632-2645.
17. Yang, Meng, et al. (2014). "Novel Heterotetrameric Enzymes in Cholesterol Metabolism from Mycobacterium tuberculosis." Protein Science. **23**: 201-201.
18. Wipperman, M. F., et al. (2013). "Shrinking the FadE proteome of Mycobacterium tuberculosis: insights into cholesterol metabolism through identification of an alpha2beta2 heterotetrameric acyl coenzyme A dehydrogenase family." J Bacteriol **195**(19): 4331-4341.

19. Yang, X., et al. (2009). "Cholesterol metabolism increases the metabolic pool of propionate in Mycobacterium tuberculosis." Biochemistry **48**(18): 3819-3821.
20. Ramakrishnan, L. (2012). "Revisiting the role of the granuloma in tuberculosis." Nat Rev Immunol **12**(5): 352-366.

Appendix

Number	Rv number	Gene name	Vector	Tag-position	Antibiotic
1	Rv3538	*hsd4B*	pET28b	N-terminal	kanamycin
2	Rv1935c	*echA13*	pET28b	N-terminal	kanamycin
3	Rv3516	*echA19*	pET30b	N-terminal	kanamycin

Table A-1. Plasmids

	Gene Name	Primers	Restriction Enzyme	DNA sequencing
1	*hsd4B*	f: 5'-TATTATCATATGCCCATCGACTTGGACGTCGCGCTGGGT-3' r: 3'-ATAATAAAGCTTCTATGCCGGCACCAGCTCCACTCCGC-3'	NdeI; HindIII	Yes
2	*echA13*	f: Constructed by Dr. Matthew Wipperman r: 5'-ATATATAAGCTTTCAGGGCCGCTGCTTGATCGCG – 3'	r: HindIII;	No
3	*echA19*	Constructed by Dr. Natasha Nesbitt		

Table A-2. Primers for recombinant enzyme constructs

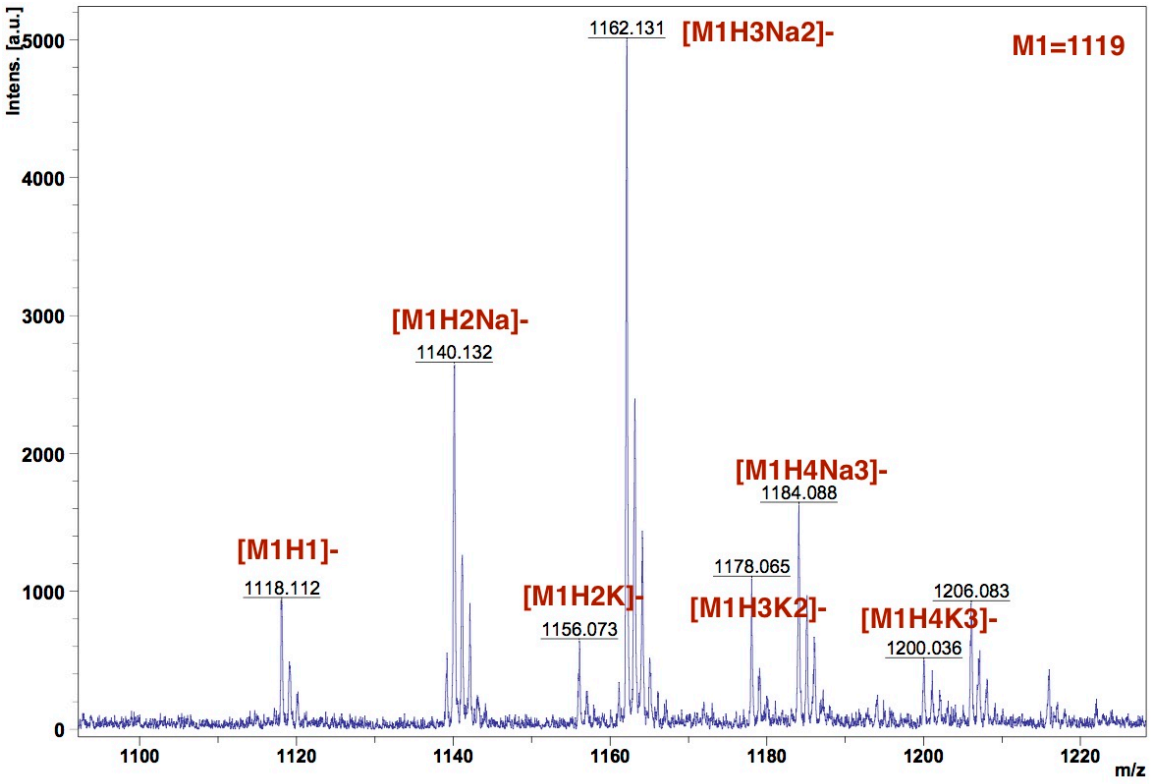

Figure A-1. MALDI-TOF mass spectrum of the control reaction of unsaturated 3-OCO-CoA (12 μM) without Rv3538

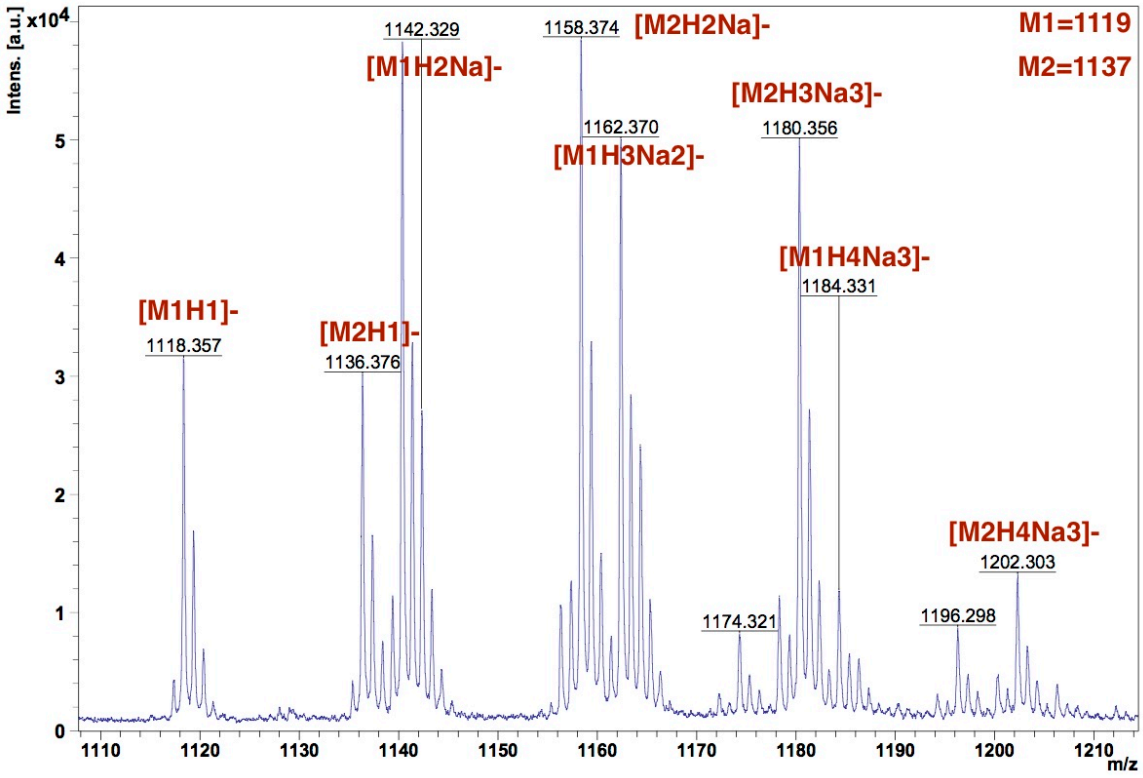

Figure A-2. MALDI TOF mass spectrum of the enzymatic reaction product of Rv3538 and unsaturated 3-OCO-CoA

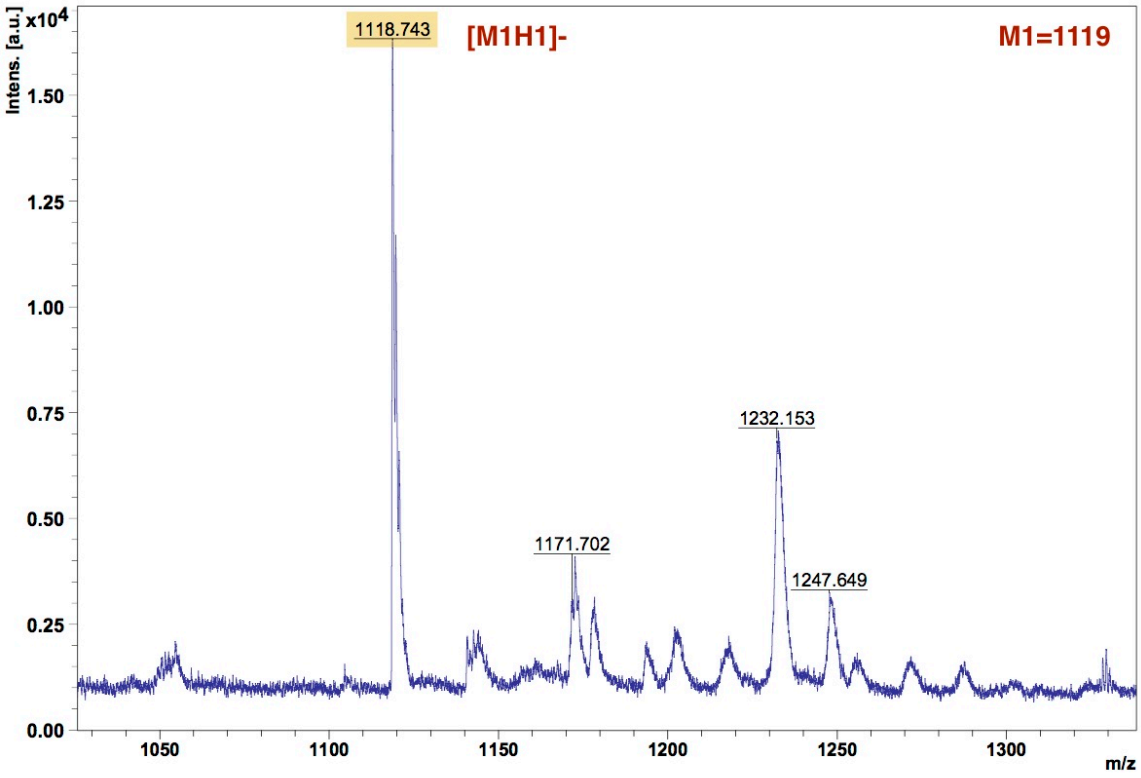

Figure A-3. MALDI TOF mass spectrum of the control reaction of unsaturated 3-OCO-CoA (25 μM) without EchA19

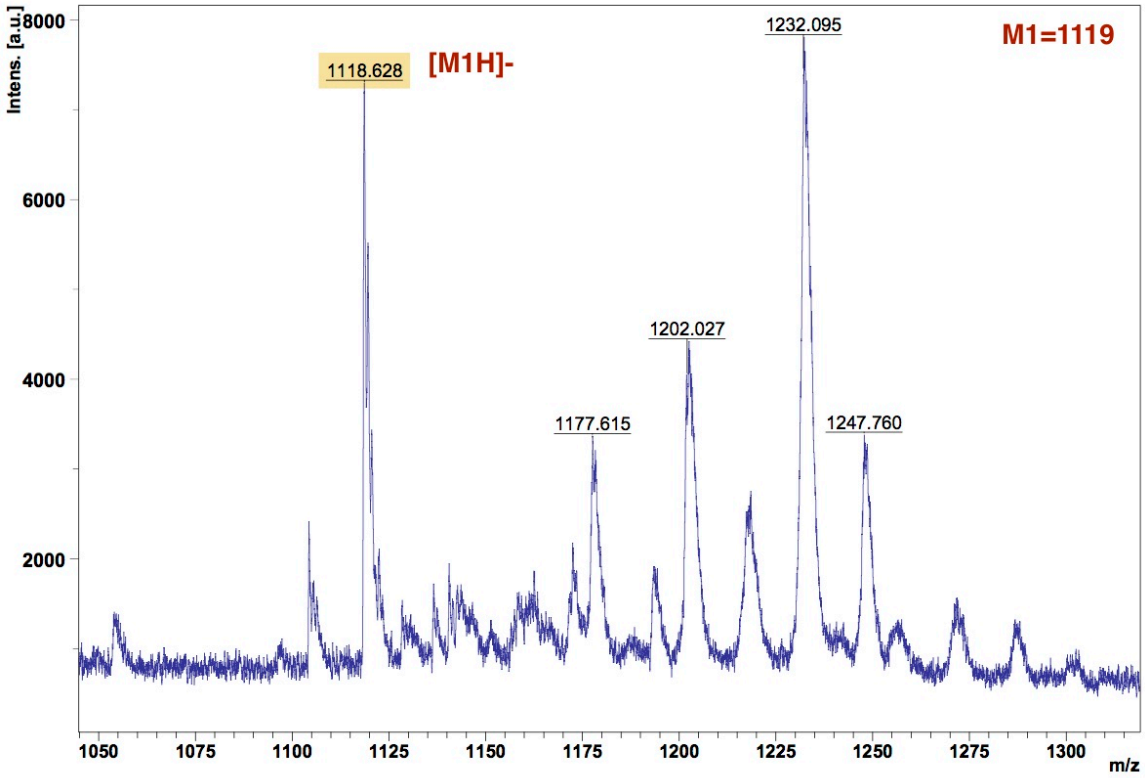

Figure A-4. MALDI TOF mass spectrum of the enzymatic reaction product of EchA19 (1 μM) and unsaturated 3-OCO-CoA (25 μM)

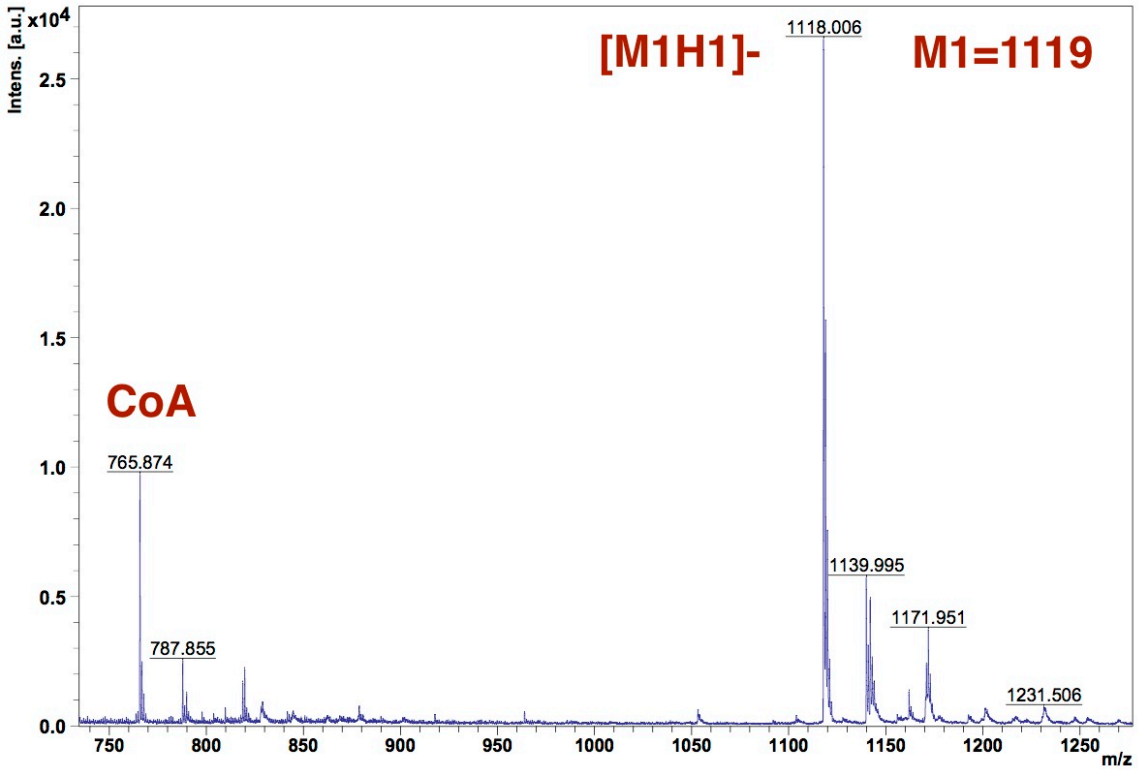

Figure A-5. MALDI TOF mass spectrum of the control reaction of the unsaturated 3OCO-CoA (25 µM) without EchA13

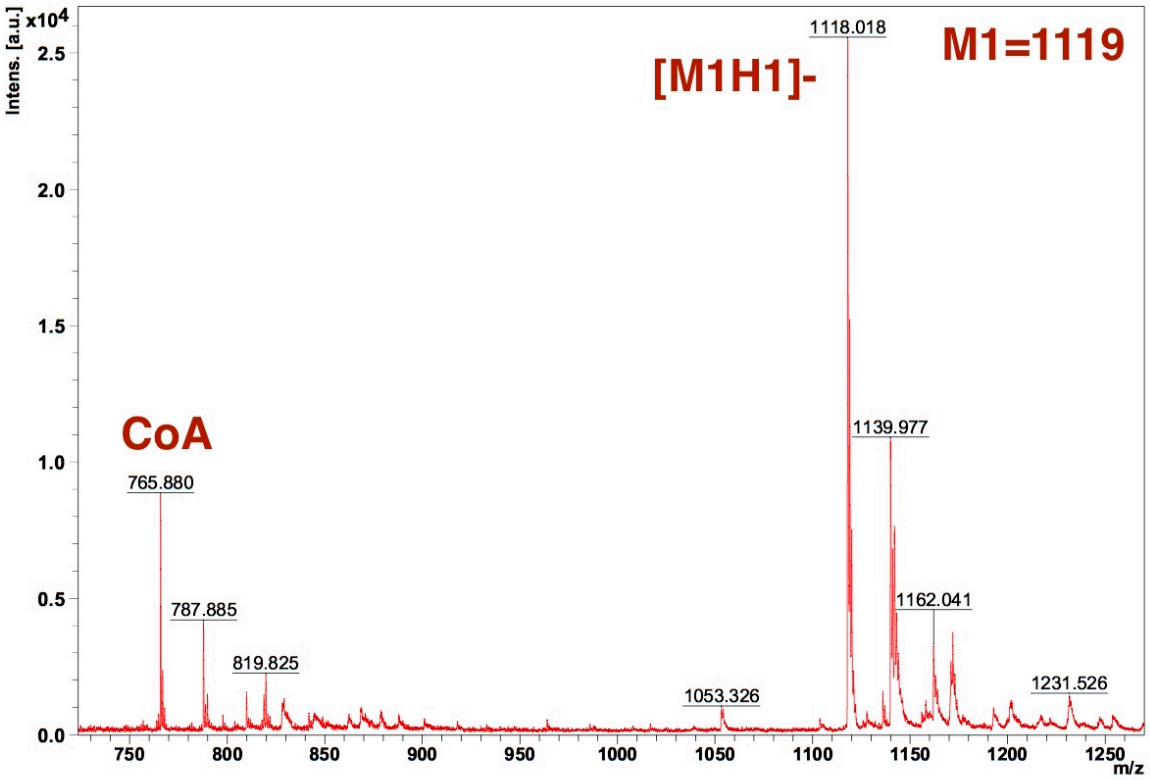

Figure A-6. MALDI TOF mass spectrum of the enzymatic reaction of EchA13 (1 μM) and the unsaturated 3-OCO-CoA (25 μM)

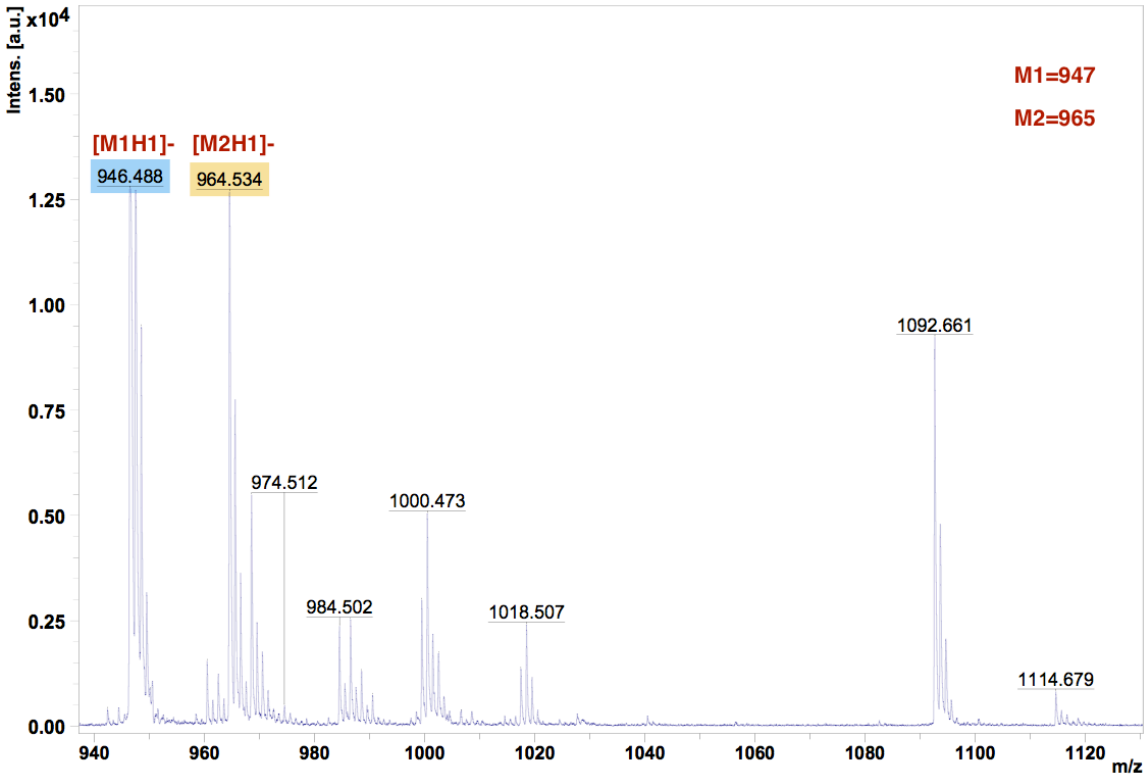

Figure A-7. The MALDI TOF mass spectrum for the starting material of 25 µM C12-enoyl-CoA

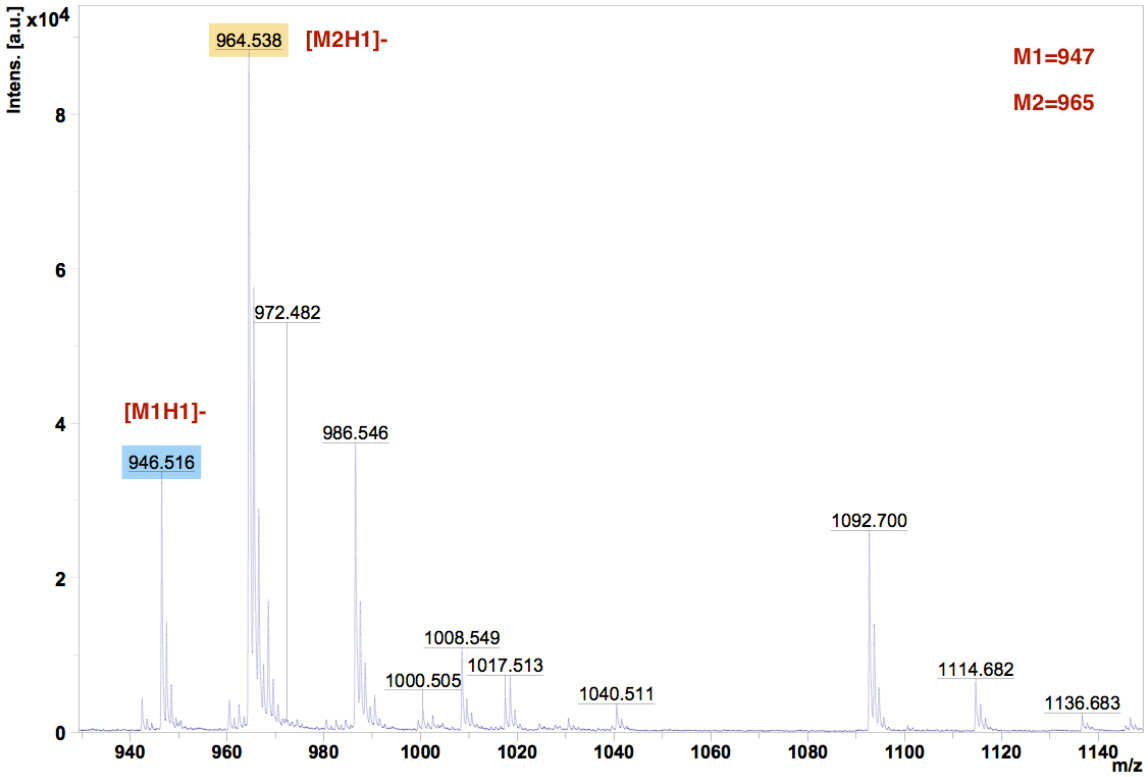

Figure A-8. The enzymatic reaction of C12-enoyl-CoA (25 µM) and EchA13 (1 µM): The hydrated product became a major compound in the mixture of the unsaturated and hydrated C12-enoyl-CoA.

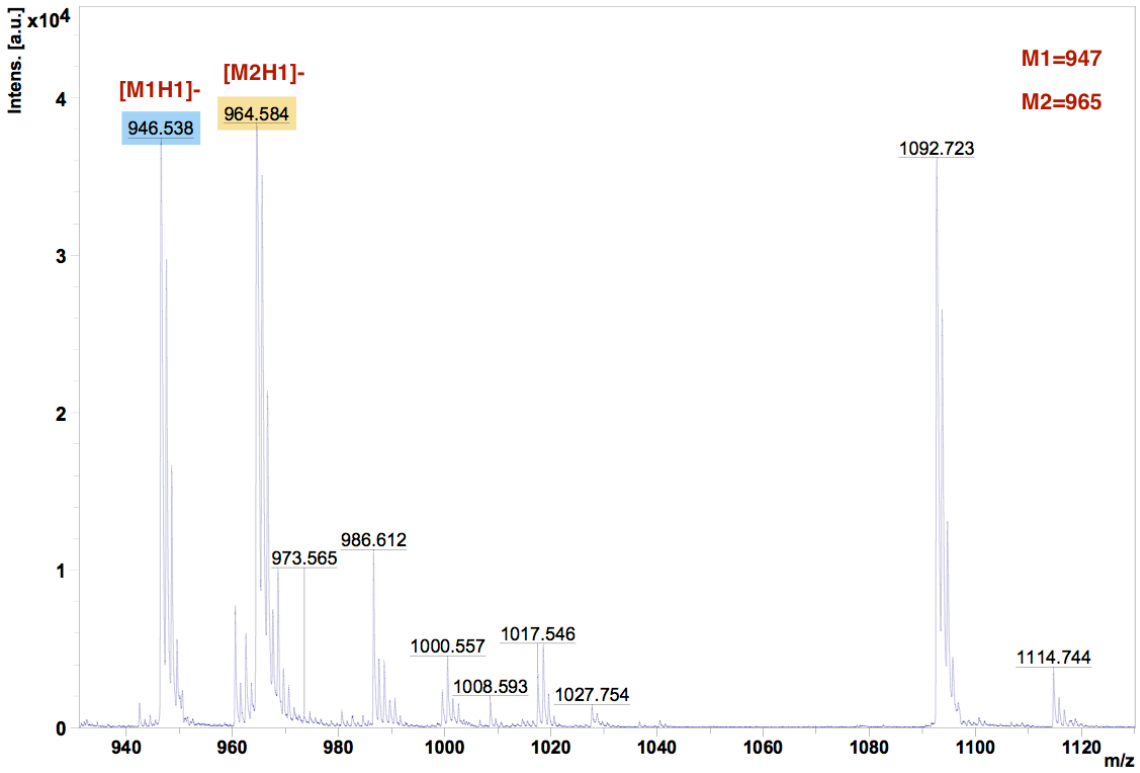

Figure A-9. The MALDI TOF mass spectrum of the solution that contains C12-enoyl-CoA (25 μM), the reaction product of C12-enoyl-CoA and EchA13, and the remaining EchA13 before the incubation: The ratio of the peak intensities at 946.538 m/z to 964.584 m/z was 1:1.

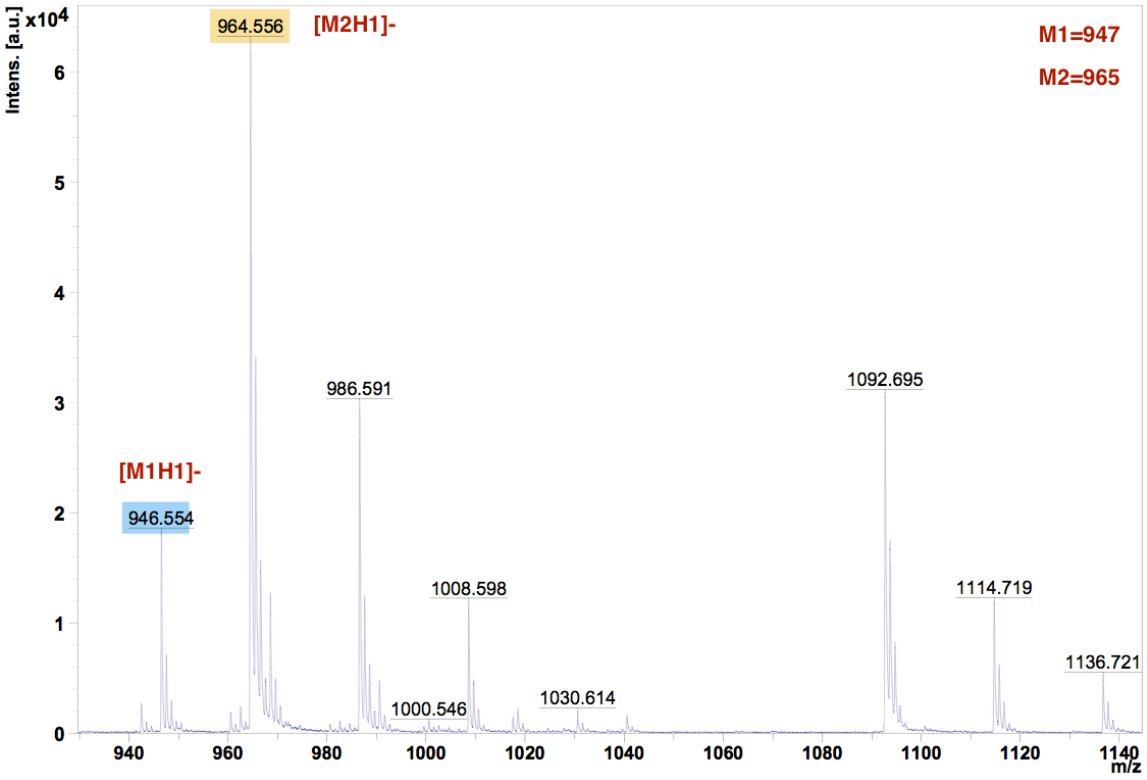

Figure A-10. The MALDI TOF mass spectrum of the incubated reaction of the extra C12-enoyl-CoA, the enzymatic reaction product, and the remaining echA13: The ratio of the intensities at 946.554 to 964.556 (m/z) was 1:3.

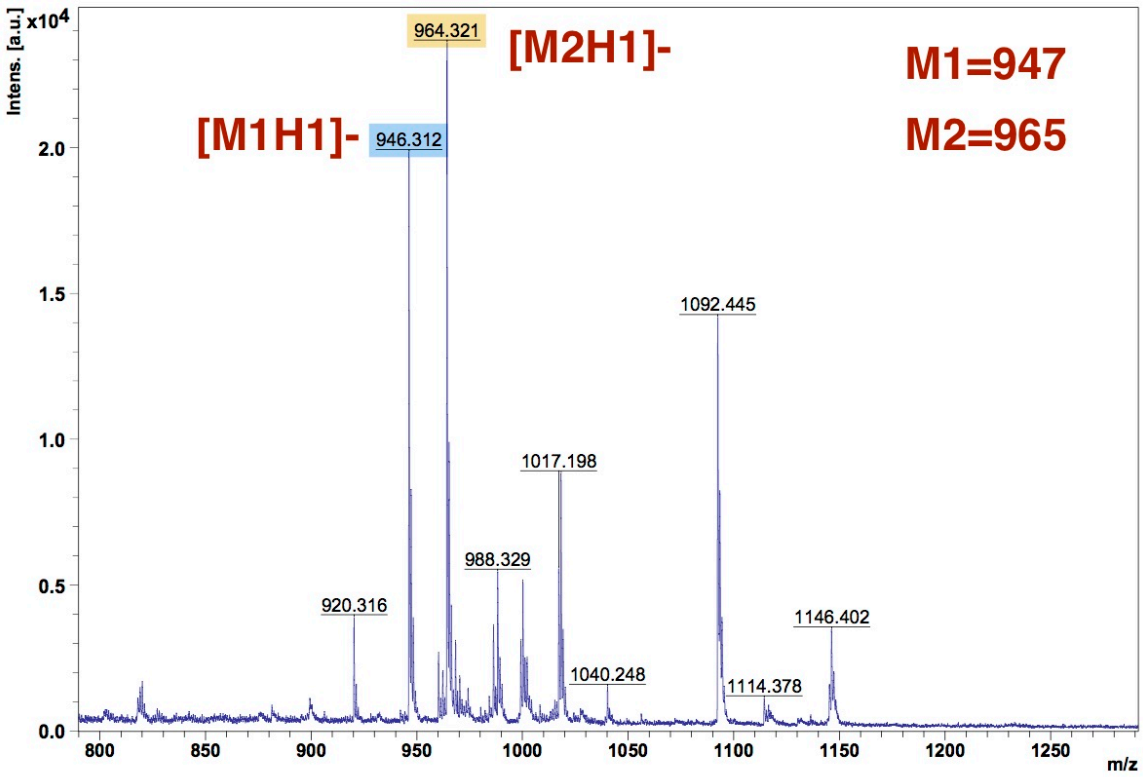

Figure A-11. MALDI TOF mass spectrum of the control reaction of C12-enoyl-CoA without EchA19

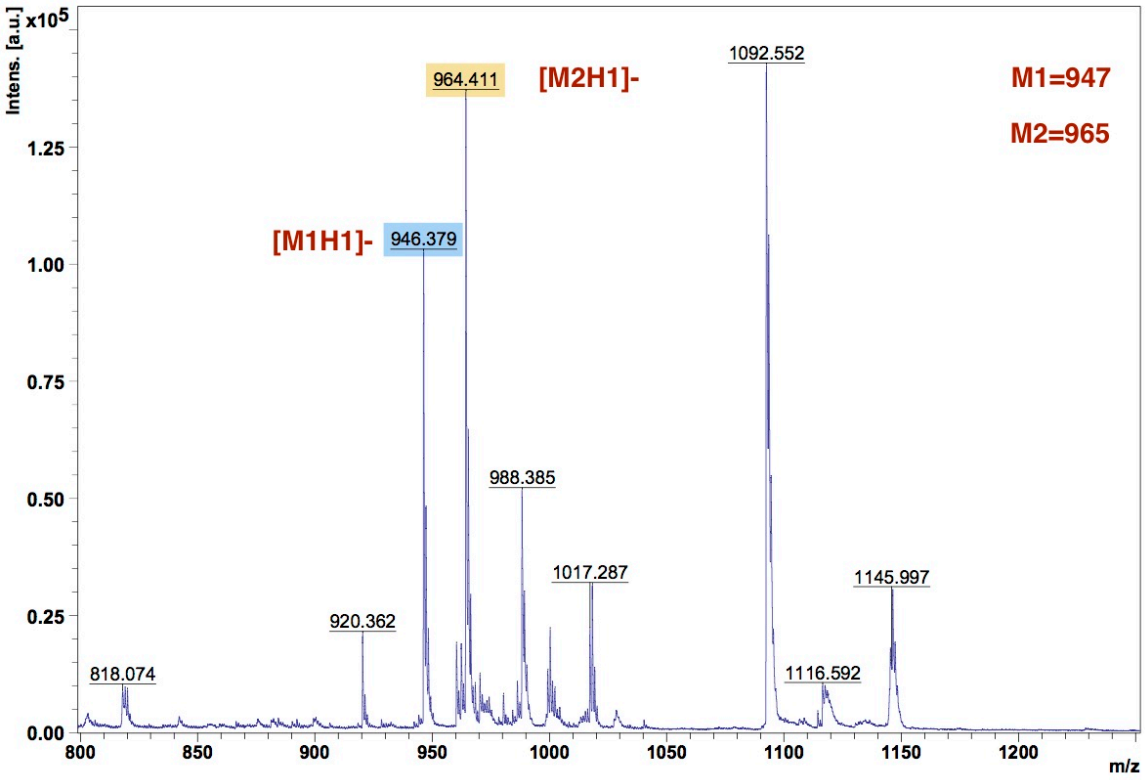

Figure A-12. MALDI TOF mass spectrum of the enzymatic reaction of C12-enoyl-CoA (25 μM) and EchA19 (1 μM)

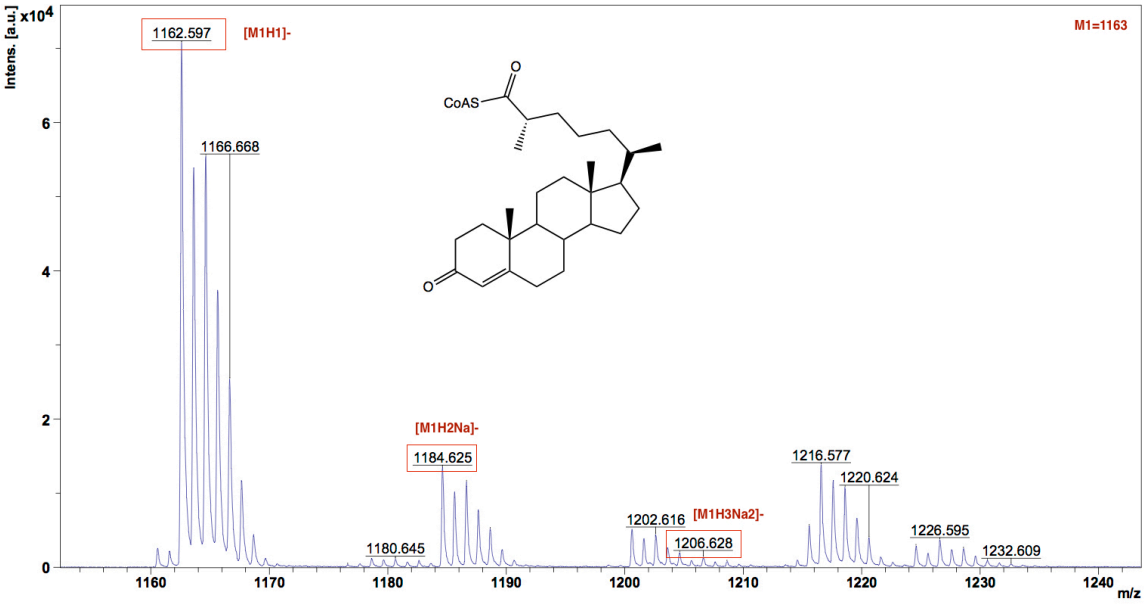

Figure A-13. The MALDI TOF mass spectrum of 3-OCS-CoA as a control reaction: the peak at 1162.597 m/z represents the saturated 3-OCS-CoA.

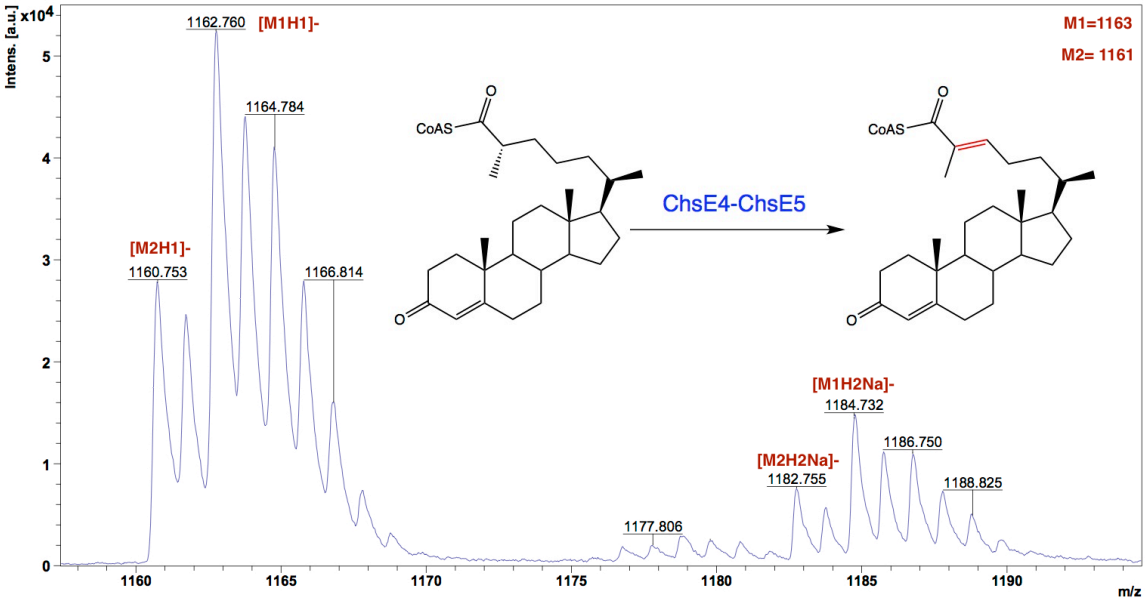

Figure A-14. The MALDI TOF mass spectrum of the reaction product of 3-OCS-CoA and ChsE4-ChsE5: The peak of the dehydrogenated 3-OCS-CoA was observed after adding ChsE4-ChsE5.

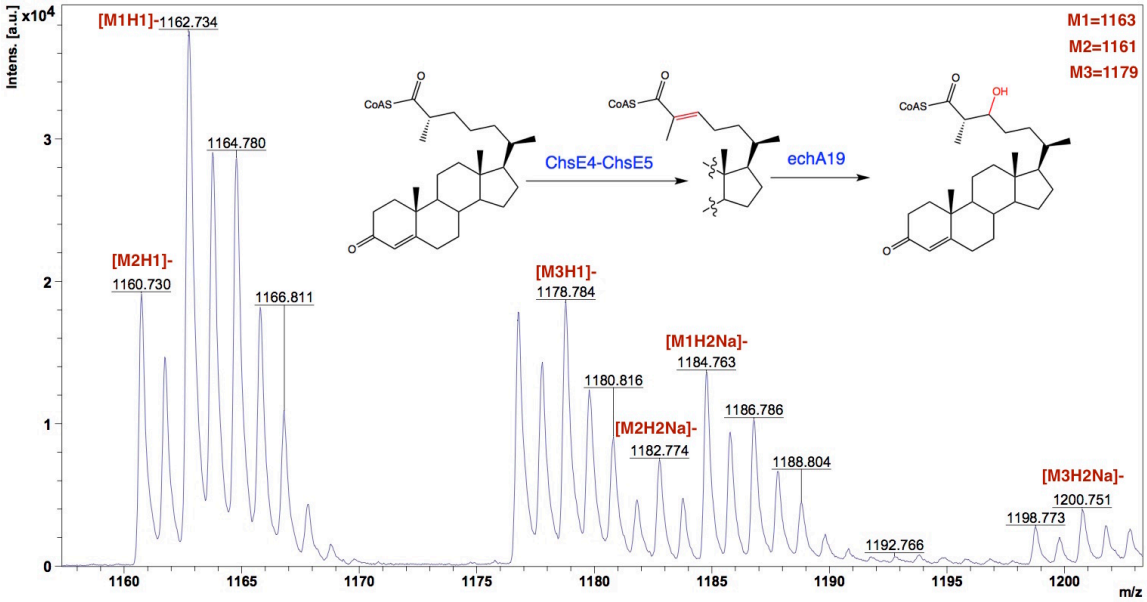

Figure A-15. The MALDI TOF mass spectrum of the reaction product of unsaturated 3-OCS-CoA and EchA19: the unsaturated 3-OCS-CoA was hydrated by EchA19.